Journal of
Marine Science and Engineering

MDPI

Article

Projected Trends in Wave Energy Potentials along the European Coasts and Implications for Wave Energy Exploitation (1976–2100)

Irene Simonetti * and Lorenzo Cappietti

LABIMA, Department of Civil and Environmental Engineering, School of Engineering, Università Degli Studi di Firenze, 50139 Firenze, Italy; lorenzo.cappietti@unifi.it
* Correspondence: irene.simonetti@unifi.it

Abstract: In the context of the efforts toward the technological development of wave energy converters, reliable estimations of the annual energy production that can be attained with a given device are fundamental for a sound evaluation of the related levelized cost of energy, which is crucial in the investment decision-making process. The lack of reliability in estimates of devices productivity can, in turn, be exacerbated by uncertainty in the available wave energy resource. The Climate Data Store of the Copernicus Climate Change Service delivers hindcast data and projections of the wave climate along the 20 m bathymetric contours of the whole European coastline, covering the periods 1976–2017 and 2040–2100. This work addresses the presence of long-term trends in wave power and the effect of these trends on wave energy exploitability and on the energy production of different wave energy converters to be installed along the Mediterranean, North African, and European Atlantic coastlines. The results show that the monthly variation in the wave energy resource will generally increase for most of the considered areas, up to double the current values in some locations. Wave energy converters will have to face more severe wave conditions, with relevant implications in terms of survivability. At the same time, the future annual energy production of the analyzed devices is expected to increase in many areas in the Mediterranean Basin (particularly in the nearest future scenario), as well as in the Baltic Sea and along the coasts of the UK and France and the north coasts of Spain.

Keywords: climate change trends; wave climate trends; wave energy converters; OWC; Aquabuoy; Langlee; OEbuoy; AWS; annual energy production

Citation: Simonetti, I.; Cappietti, L. Projected Trends in Wave Energy Potentials along the European Coasts and Implications for Wave Energy Exploitation (1976–2100). *J. Mar. Sci. Eng.* **2024**, *12*, 239. https://doi.org/10.3390/jmse12020239

Academic Editor: Eugen Rusu

Received: 27 December 2023
Revised: 23 January 2024
Accepted: 24 January 2024
Published: 29 January 2024

1. Introduction

In coastal areas, sea-level rise and coastal storms are listed among the main drivers of climate-related hazards in the framework of climate change. Climate change could have clear effects on sea waves, directly influencing the variables that determine their generation and propagation towards the shore (e.g., wind speed and direction, sea ice cover). The Intergovernmental Panel on Climate Change (IPCC, [1]) delivered projections of climate scenarios induced by different trends in the emissions of Greenhouses Gases (GHC), defined as Representative Concentration Pathways (RCPs). Among these, RCP8.5 represents a worst-case scenario with 8.5 $W \cdot m^{-2}$ of radiative forcing, which would be caused by a stable increase in GHG emissions up to 2100. Low-emission technologies could aid in mitigating climate change. The International Energy Agency [2] foresees that approximately 45% of the decrease in CO_2 emissions by 2050 could be obtained by technologies that are, at present, in the development stage. There is, therefore, a two-way relationship between climate and the exploitation of renewables: renewables are needed to mitigate the changes, and in turn, the performance and survivability of renewable energy converters will be unavoidably affected by climate change. This may pose issues for both new designs of conversion plants and for already installed ones. The potential of marine

renewable energies (MREs) to promote the transition towards cleaner energy sources is well recognized [3], with the offshore wind global installed capacity expected to increase up to thirty-fold in the upcoming decades and wave energy and tidal energy potentially contributing up to 10% of the global energy demand [4]. Despite the potential of wave energy conversion and the wide research efforts towards its technological development in recent decades, the technology is still de facto confined to a pre-commercial stage, due to different technical and non-technical issues. Among those, key challenges are the improvement of the overall lifetime, reliability, installability, operability, and maintainability of wave energy converters (WEC). Overcoming these challenges would ultimately lead to the reduction of the Levelized Cost of Energy (LCOE) to values comparable to those of more diffused technologies for energy conversion.

In this context, a solid understanding of the wave resource variation under climate change is crucial to ensure the performance and survivability of the devices to be installed in the upcoming decades. Over the last few years, the topic of identifying the long-term effects of climate change on ocean waves has been addressed in several studies, regarding both:

1. The identification of trends in historical multi-decadal wave data (e.g., at the global scale [5–10] and at the regional scale of the Mediterranean Basin [11–14]);
2. The projection of the future wave climate up to the end of the century in a climate change context (e.g., at the global scale: [15–19] and at the Mediterranean Basin-scale: [20–22]).

For both of the aforementioned categories of study (hindcast or projections), the robustness of the estimated long-term trends in the wave characteristics still needs to be improved. Indeed, even if wave data from hindcasting or reanalysis are usually judged as accurate, inhomogeneities introduced during the process of assimilating observations may induce uncertainty in the long-term trends [16].

Recently, De Leo et al. [23] reviewed the existing studies addressing trends in historical wave data in the Mediterranean Sea, observing that previous studies identified either increasing or decreasing significant trends with a similar frequency of occurrence over the different Mediterranean sub-basins. Analyzing hindcast data for the Mediterranean Basin, Barbariol et al. [12] also pointed out different long-term trends in the summer and winter seasons for both mean and extreme wave values (with decreasing trends in the summer and increasing trends in the winter in several locations). Overall, previous studies showed a limited consensus concerning the expected trends in different wave integral parameters. As far as projections of the wave climate for the upcoming decades are concerned, a relatively high agreement exists on the expected change in mean annual values: the most recent studies by Bernardino et al. [18] and Meucci et al., 2023 [19] (with forcing of wind speed and sea ice cover data from the CIMP5 [24] and CIMP6 [25] models, respectively, both under RCP8.5 projections to 2100) further confirmed the foreseen increases in the mean significant wave height and average wave energy in the South Atlantic, and the decrease in the North Atlantic and Northwestern Pacific ocean found in the previous studies [26,27]. The trend in extreme events has, instead, a greater uncertainty, except for consistent projections of an increase for the Southern Ocean and a decrease for the North Atlantic area [15,16,26].

Studies of the projected wave climate under the RCP8.5 scenario in the Mediterranean Sea [20] show a decreasing trend for annual mean and maximum values of significant wave height and mean periods over most of the Mediterranean Basin. Lobeto at al. [17] highlighted a moderate (<1 m) increase in the wave height with a return period of 20 years in the western Mediterranean area and an opposite decrease in the eastern Mediterranean Sea. In contrast, annual mean values of significant wave height were found to decrease over most of the basin. The divergence in the trends for mean and extreme wave conditions for the Mediterranean basin has been confirmed also in [22], where a general tendency towards more geographically dispersed trends in annual maxima compared to lower percentiles of wave characteristic parameters is observed. Concerning the wave energy resource, significant increasing trends are observed for the mean annual wave power in the Alboran

Sea, along most of the western coasts of Italy and the Aegean coasts of Croatia, Greece, and Albania [22].

Only a few studies attempted to evaluate the effect of possible modifications in the wave climate on the power production of WECs. Ulazia et al. [28,29] addressed the issue of the difference in the optimal geometry of an Oscillating Water Column (OWC) device over the four decades between 1979 and 2018 in selected geographical locations along the North-East Atlantic Ocean areas of Europe and Africa. The authors found significant differences between the original device geometry and that optimized accounting for the expected future modifications of the wave climate. These differences in the optimal geometry reach a maximum of 15% in some locations, with a variation of up to 20% in the annual energy production of the device, suggesting the need for a long-term perspective in the sizing and development of possible control strategies for WECs. Simonetti & Cappietti [22] evaluated the effects of long-term changes in the wave climate, as projected in the RCP8.5 IPCC scenario, on the optimal dimensions and power production of OWC devices along the whole Mediterranean Sea coastline. Relative variations of up to 10% in the optimal size of the OWC chamber and applied damping were found, with increases in the annual power production in most of the locations considered. Slight modifications in the optimal geometry of a hypothetical OWC for the installation along the Atlantic European coastlines were also found [30].

In this work, we extend the study presented in [22,30] to consider the effect of long-term changes in the wave power on the potential for wave energy exploitation along European coasts, also considering the possible variation in the performance of a set of state-of-the-art devices. The remainder of the paper is structured as follows: the wave data used to characterize the present and future wave climates and the related trends are presented first, followed by the discussion of the indexes used to assess the variation in the wave energy exploitability and WEC selected for the comparison of performance in the present and future scenarios. Results are then presented and discussed.

2. Methodology

2.1. Wave Data Projections and Trend Analysis

The present study uses the data delivered by the Copernicus Climate Change Service, through the Climate Data Store (CDS) [31]. This dataset contains wave data for the whole of the European and North African coastlines (at a water depth of 20 m), with a resolution of ∼30 km in space and 1 h in time, and includes the following scenarios:

- A historical reanalysis based on ERA5 data (for the period 1976–2017), which is the most recent reanalysis of the global climate and weather at the European level, provided by the European Centre for Medium-Range Weather Forecasts (ECMWF) [32];
- Two projected scenarios corresponding to RCP4.5 and RCP8.5 as defined by the IPCC (for the period 2040 to 2100), which uses the wind forcing from the HIRHAM5 Regional Climate Model.

In these scenarios, the CDS service of Copernicus delivers data produced by ECMWF by using the third-generation wave model WAM. The model solves the wave action balance equation on arbitrary water depths, including the processes of wave generation by wind, wave advection, wave dissipation due to white capping and bottom friction, shoaling, and refraction, which impact wave transformation from deep to shallow water [33]. In particular, a stand-alone version of the wave model WAM, denoted as SAW, was used to produce the CDS's data. The results of the SAW model have been satisfactorily calibrated and validated [34]. It has to be mentioned that the global wave power derived from the ERA5 reanalysis database has recently been independently validated also with satellite altimeter observations and shown to have limited bias [10].

At the latest access to the data used for this study, the CDS dataset contained the spectral peak period T_p only. For this reason, the period $T_{m-1,0}$ (i.e., the so-called energy

period) is obtained from the T_p by assuming a given shape of the wave energy spectrum, allowing us to obtain

$$T_{m-1,0} = \alpha \cdot T_p \quad (1)$$

For a JONSWAP spectrum with a peak enhancement factor $\gamma = 3.3$, we obtain $\alpha = 0.904$. For each grid point along the whole of the Atlantic coasts of Europe and North Africa, the available time series of wave data have been analyzed to assess the presence of trends in the variation in the available wave power P_{wave}, computed as Equation (2).

$$P_{wave} = \frac{1}{16}\rho \cdot g \cdot H_{m0}^2 \cdot C_g \quad (2)$$

where ρ is the water density, g is gravitational acceleration, and C_g is the wave group velocity (obtained by applying the linear dispersion relation at the given water depth h, by using the wave period $T_{m-1,0}$). It is known that Equation (2) provides an approximation of the exact wave power of irregular waves of a given spectrum on finite water depth, but the errors caused by this approximation, compared to the exact solution, were found to be negligible on the assessment of the wave power [35]. The trends in the annual mean value and in the annual maxima of the wave power P_{wave} are analyzed over the whole dataset (i.e., for the period 1976–2100). The following indexes are used to evaluate the presence of trends in the wave data, which are among the most diffused for studying the significance of climate trends: (i) the Theil–Sen's slope s [36], a non-parametric and robust estimator of the trend in sample data; (ii) the p-value of Mann–Kendall tests [37], which is a non-parametric test used to identify the presence of a trend in a series. The null hypothesis is the absence of a trend: p-values close to 1 denote that data are consistent with the null hypothesis, while p-values close to 0 are an index of a significant trend.

2.2. Wave Energy Exploitability Indexes

To further analyze the possible impact of the projected changes in the wave climate on wave energy exploitability, some of the indexes traditionally used in the literature to identify the most suitable locations for WECs installation (e.g., [38–41]) have been considered in the present work. The variability in time of the available wave energy is one of the pivotal factors for the selection of exploitable sea sites, in terms of higher average values and higher time stability of the wave energy resource. A more stable wave energy resource makes it easier to obtain a sizing of the nominal power of the device which maximizes the ratio of the produced annual energy to the WEC's cost. To evaluate the variability in the wave energy at the intra-annual scale, in both the present and the projected future climates, the short-term stability of the resource was evaluated through the Monthly Variability Index (MVI) [38,41,42], which expresses the ratio of the difference between the maximum and minimum mean monthly wave power to its annual mean. In the present (P, period 1986–2016) and future scenarios (F1 and F2, 2040–2070 and 2070–2100, respectively), the indexes (MVI_P, MVI_{F1}, and MVI_{F2}) are computed as the average values of annual MVI over the related time window.

The Wave Energy Development Index (WEDI) [38,40], expressing the ratio of the mean annual wave power $\overline{P_{wave}}$ to the maximum annual power P_{wave}^{max}, is also analyzed. The WEDI is considered an index of the severity of the installation area: lower values of WEDI denote areas in which a WEC has to withstand a high level of wave power during the most energetic storms relative to the average operating conditions for wave energy extraction. Conversely, regions with a high mean value of wave power and a low maximum denote a high energy potential without penalizing the WEC survivability and are associated with high values of WEDI. In each location, the WEDI representative of present (P) conditions has been obtained based on hindcast data relative to the period 1986–2016. In particular, yearly values of WEDI were computed as in Equation (3), and then averaged over the reference period to provide a representative value $WEDI_P$. In the same way, projected

future values (F1 and F2) of WEDI were computed for the period 2040–2070 ($WEDI_{F1}$) and the period 2070–2100 ($WEDI_{F2}$).

$$WEDI = \frac{\overline{P_{wave}}}{P_{wave}^{max}} \quad (3)$$

The variations in MVI and WEDI in scenarios F1 and F2, relative to scenario P, are computed as follows:

$$\Delta MVI = \frac{MVI_{F1/F2} - MVI_P}{MVI_P} \quad (4)$$

$$\Delta WEDI = \frac{WEDI_{F1/F2} - WEDI_P}{WEDI_P} \quad (5)$$

2.3. Evaluation of Present and Future WEC Performance and Selection of Power Matrices of the Devices

In each location along the 20 m bathymetric contour of the Mediterranean, Atlantic European, and North African coasts, the wave climate of the present and future scenarios has been characterized in terms of scatter matrix (SM), obtained based on 30 years of wave data (scenario F: 1986–2016, scenario P1: 2040–2070, and scenario P2: 2070–2100). SMs are discretized in bins of 0.25 m (for H_{m0}) and 0.25 s (for $T_{m-1,0}$), and represent the probability of occurrence of the given H_{m0} and $T_{m-1,0}$ pair. To provide a first estimation of the effect of variations in the wave climate on the productivity of WECs, we computed the Annual Energy Production (AEP) of a set of devices for the present and future SMs. The relative variation in the AEP of each device in the future scenarios F1 and F2 is computed as:

$$\Delta AEP = \frac{AEP_{F1/F2} - AEP_P}{AEP_P} \quad (6)$$

The WECs are characterized in terms of power matrix (PM), which shows the average power production of the device for a given couple of H_{m0} and $T_{m-1,0}$. Different WEC technologies were considered in the present work (Table 1), using as selection criteria: (i) the technologies reached a high development stage, with tests at the sea and the resulting performance data are freely available in the form of PM; (ii) the WECs work bases on different principles; and (iii) the devices have been widely used in the literature for benchmarking purposes and studies concerning the exploitability of the wave energy in different locations worldwide (e.g., [43–47]). Based on such criteria, the following devices were selected:

- The AquaBuoy [48,49] (Finavra Renewables Ocean Energy Ltd., London, UK) is a floating buoy point absorber, reacting against a submersed water mass contained in a reaction tube, with both its ends open and a hose pump attached to each end, which moves in heave with the waves. The hose pump compresses the water, driving the water flow through a Pelton turbine, connected to a generator;
- The Archimedes Wave Swing (AWS) [50,51] (AWC Ocean Energy Ltd., Inverness, UK) is a heaving point absorber anchored to the seabed, composed of two interconnected concentric cylinders, with the inner one fixed to the seabed and the outer one free to move in heave as the wave passes. The Power Take Off (PTO) system consists of a linear generator;
- The Langlee [52] is s semi-submersed wave surge converter, first conceived in 2005 in Norway and developed by Langlee Wave Power Ltd., Kristiansund, Norway. It consists of four hinged flaps (with two pairs of symmetric flaps opposing each other), connected to a common frame and positioned below the mean still water level. When excited by the waves, the flaps move relative to the supporting structure;
- The fixed OWC, one of the most consolidated WEC concepts [53], consists of a hollow chamber, open below the free surface and fixed to the seabed, where the incident waves cause the heave motion of an inner mass of water, in turn compressing the air in the upper part of the chamber and driving an airflow through an air turbine.

For this device, the PM given in [51] is used, assuming a width of the OWC chamber perpendicular to the direction of wave propagation of 10 m;

- The OEbuoy is a floating OWC device, initially developed in 2007 by OceanEnergy Ltd., UK [54]. Similarly to its fixed version, the wave energy compresses the air in a plenum chamber and drives an air turbine. In this specific WEC concept, the mouth of the device opens in the opposite direction relative to the incident waves.

It is worth stressing that the PMs of the WEC technologies used in this work are derived from devices conceived or optimized for relatively highly energetic sea states, e.g., those of the European Atlantic Ocean areas. In moderate wave climates, such as that of the Mediterranean Sea, such devices may be oversized [45] and would require a specific sizing for performance optimization [22,55]. Such analysis is outside the scope of the present work, which mainly aims at a relative evaluation of variations in device performance in the present and future wave climate.

Table 1. Technical specifications of the WEC systems considered in the present work and reference for the related Power Matrix (PM).

Device	Device Type	PTO/Rated Power [kW]	Ref. for PM
AquaBuoy	Point absorber	Pelton turbine/250	[48]
AWS	Heaving point absorber	Linear generator/2500	[50]
Langlee	Oscillating wave surge	Direct mechanical drive/1665	[56]
OWC	Fixed OWC	Air turbine/85	[51]
OEbuoy	Floating OWC	Air turbine/2880	[56]

3. Results

Trends in the mean annual wave power and the maximum annual wave power are analyzed in this section, considering projections in the CDS database under RCP8.5 only and for data covering the whole available period (1976–2100). Subsequently, for the same emission scenario, indexes for wave energy exploitation are compared in the present and future wave climate (scenarios P, F1, and F2 as described above), and finally, the expected changes in the annual energy production of the selected WECs are evaluated.

3.1. Trends in the Mean and Maximum Wave Power

Trends in the annual mean values of specific wave power, $\overline{P_{wave}}$, in the Mediterranean Basin have been discussed in [22], and are just briefly recalled here for the sake of completeness. Highly significant (i.e., with p-values close to zero) increasing trends are observed in the Alboran Sea, and along most of the western coast of South Italy and the coasts of Croatia, Greece, and Albania in the Aegean Sea (Figure 1a,b). In such areas, the maximum s-values reach around 0.01 kW/m per year. Conversely, significant decreasing trends (up to about -0.01 kW/m per year) characterize the eastern Levantine Sea. The increase in the wave power in the Alboran Sea, near the Strait of Sicily and north of Crete, in the Aegean Sea, is consistent with the previous study by Loarca et al. [21], particularly for the nearest future scenario (2040–2070).

For the Atlantic Coasts of Western Sahara, Morocco, and Portugal (latitudes between 25° N and 44° N) projected data in the CDS database for RCP8.5 scenarios (Figure 1c,d) show a vast majority of decreasing trends in $\overline{P_{wave}}$ (with Theil–Sen's s-values up to -0.025 kW/(m·year) in the South of Morocco and the Azores). Considering the p-value of the Mann–Kendall test (Figure 1d), the aforementioned trends seem highly significant (i.e., p-value close to 0) along most of the Western Sahara, Morocco, and for the Azores. Decreasing trends, with s-values between -0.005 and -0.01 kW/(m·year), are seen along the North of the coast of Portugal; however, for this area, the trends are scarcely significant (Mann–Kendall p-values higher than 0.4). A decreasing trend in the mean annual wave power $\overline{P_{wave}}$ is detected also on the Atlantic coasts of Spain and France and most of the western coasts of the United Kingdom and Ireland (latitudes of 42° N–62° N and longitudes -10° W to 5° E, Figure 1e,f).

Based on the Mann–Kendall test, the trends are particularly significant along the west coast of Ireland (with a maximum s-value up -0.09 kW/m·year). For higher latitudes, increasing trends in the annual average value of wave power $\overline{P_{wave}}$ are observed on most of the Baltic basin and along the northern coast of Norway (Figure 1g,h). In this area, trends are significant (with p-values in the range of 0–0.1). Scarcely significant decreasing trends in $\overline{P_{wave}}$ are observed, instead, in the south of Norway and the North Baltic Sea. The latter trends are limited in magnitude, i.e., s is lower than -0.005 kW/(m·year).

Overall, the prevailing decreasing trends in $\overline{P_{wave}}$ in most of the Atlantic coasts of Europe and North Africa between latitudes of 20° N and 60° N, as well as the increasing trend for latitudes greater than 65° N, is consistent with works in the literature [18,19].

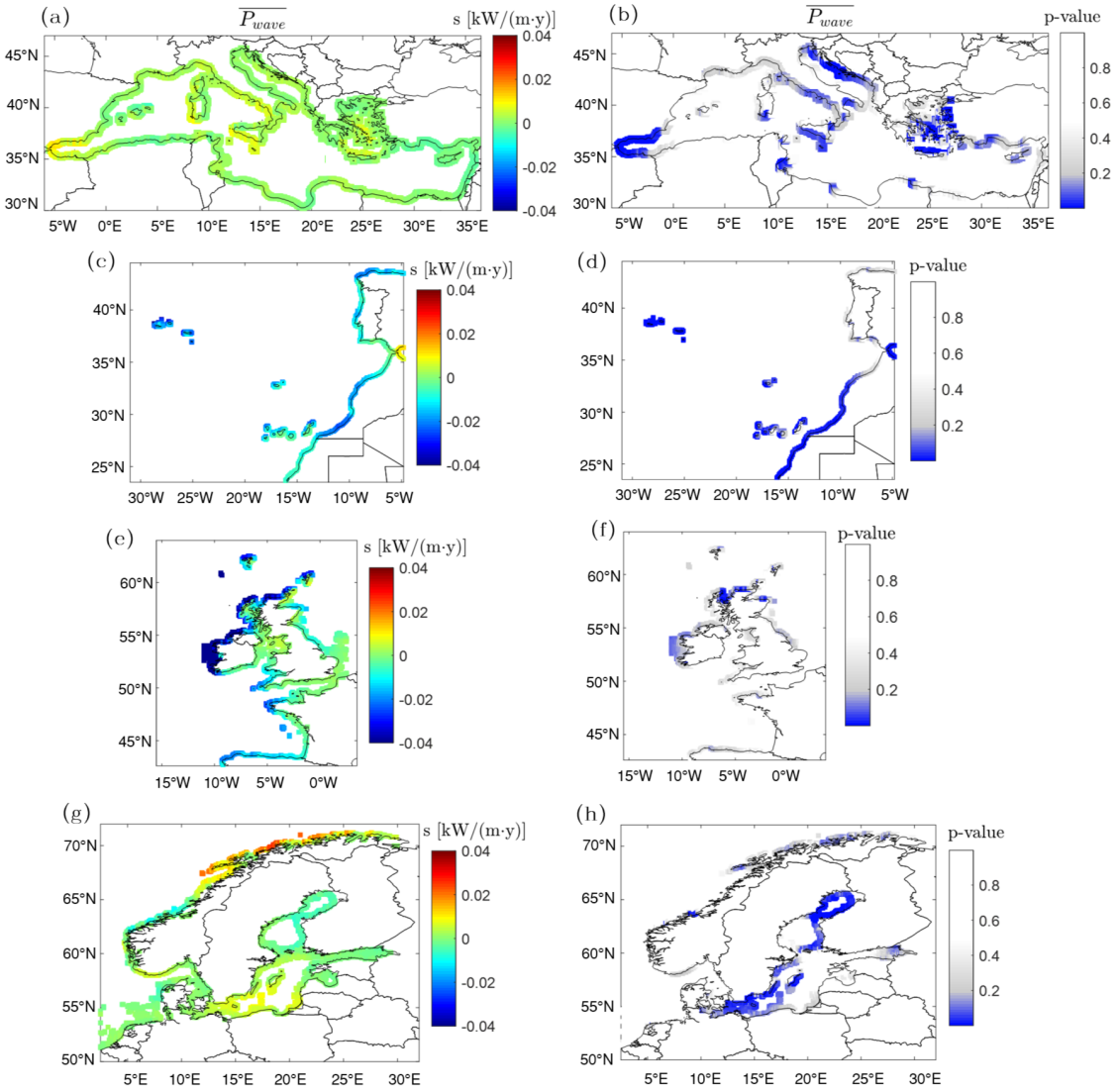

Figure 1. Spatial distribution of Theil–Sen's slope (**left**) s and p-value of Mann–Kendall test (**right**) under the RCP8.5 scenario for the annual mean wave power $\overline{P_{wave}}$: Mediterranean Basin (**a**,**b**), Atlantic coasts of Western Sahara, Morocco, and Portugal (**c**,**d**), Atlantic coasts of Spain, France, and the United Kingdom (**e**,**f**), coasts of the North, Baltic, and Norwegian Seas (**g**,**h**).

The maximum annual power P_{wave}^{max} exhibits a prevalence of increasing trends in all the considered geographical areas (Figure 2). In the Mediterranean Basin (Figure 2a,b), the greatest magnitude of the trend of around 0.6 kW/(m·year) is observed along the west coast of Corsica, the southern coast of Sicily, and the Gulf of Sirte. These trends are associated with p-values lower than 0.1, i.e., can be considered significant. Significant increasing trends

in P_{wave}^{max} (0.15–0.3 kW/m per year) are also found in the Alboran Sea and the Ligurian Sea and along most of the Tyrrhenian coast of Italy, as well as in the Adriatic and Ionian coasts of Croatia, Albania, and Greece.

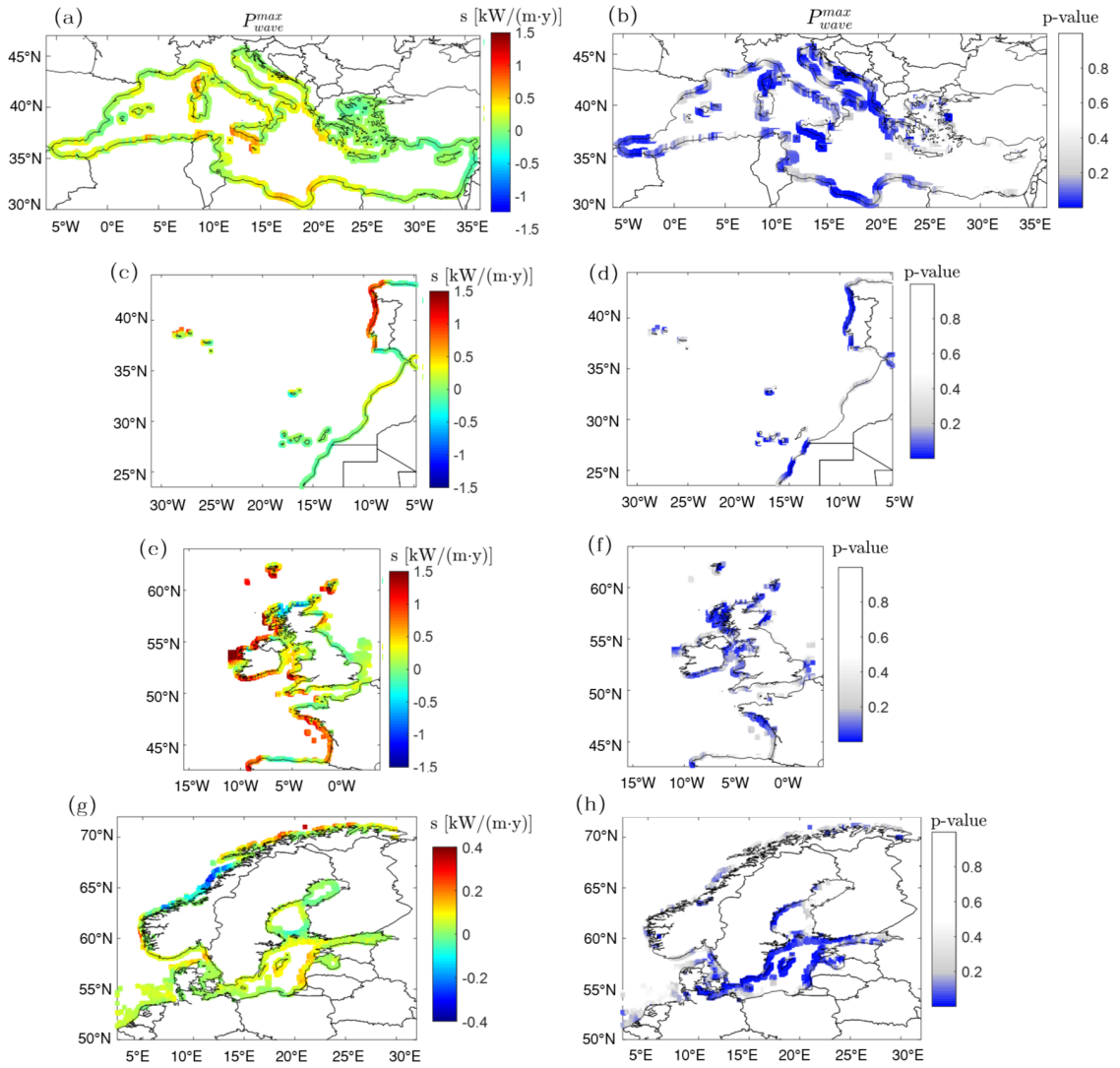

Figure 2. As in Figure 1, but for the annual maximum wave power P_{wave}^{max}.

A significant increasing trend in P_{wave}^{max} (with s-values of 0.6–1 kW/m per year) is also found along the Atlantic coast of Portugal (Figure 2c,d), while trends are scarcely significant along the Atlantic coasts of Morocco. Along Western Sahara, a significant decreasing trend in P_{wave}^{max} is observed (s-value around -0.1 kW/m per year). A significant increasing trend in P_{wave}^{max} is detected also for the western coast of France and that of the United Kingdom and Ireland (Figure 2e,f), reaching a maximum of around 1.6 kW/m per year. For higher latitudes (Figure 2g,h), a significant increasing trend is seen in the Baltic Sea (with s = 0.4–0.8 kW/m per year), while the increasing trend observable along the northern coast of Norway can be considered not significant (p-values of 0.2–0.4). The expected increase in the annual maximum values of the wave conditions for the central Baltic Basin is also confirmed in the work of [57]. The authors identified the causes of such an increase in the greater fetches available for wave generation due to ice retreating in the projected climate scenario.

A set of locations has been selected as reference points (P1–P7 in Figure 3) to show examples of the time series of $\overline{P_{wave}}$ and P_{wave}^{max} (and additionally, of the annual mean and

maximum value of the significant wave height, $\overline{H_{m0}}$ and H_{m0}^{max}, Figures 4 and 5) and to later to show the AEP of the WECs in the present and future wave climates in Section 3.3. P1, P2, and P3 are located in the Mediterranean Basin, respectively, on the west coast of Corsica, in the Ionian Sea along the coast of South Italy, and in the Gulf of Sirte. As shown globally in Figures 1 and 2, in P1, no significant trends are detected for the mean power $\overline{P_{wave}}$, while a significant increasing trend is found for P_{wave}^{max}. In P2 and P3, instead, a significant increasing trend characterizes both $\overline{P_{wave}}$ and P_{wave}^{max}.

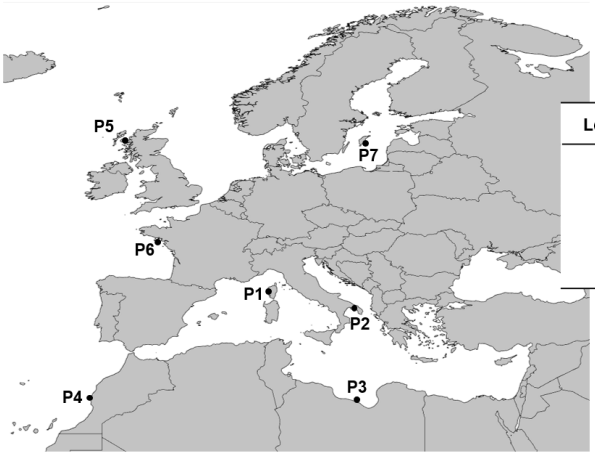

Location	Coordinates Lat., Long.	Area	Trend on $\overline{P_{wave}}$	Trend on P_{wave}^{max}
P1	42.2°N, 8.5°E	West Corse	--	↑
P2	40.3°N, 17.4°E	Ionian Sea	↑	↑
P3	30.7°N, 18.4°E	Gulf of Sirte	↑	↑
P4	31.2°N, 9.9°W	Morocco	↓	--
P5	56.3°N, 6.5°W	North UK	--	↑
P6	46.7°N, 2.4°W	West France	--	↑
P7	57.1°N, 18.7°E	Central Baltic	↑	↑

↑ increasing trend
↓ decreasing trend
-- non-significant trend

Figure 3. Locations of selected points P1–P7 and trend detected in the data delivered by the Copernicus CDS.

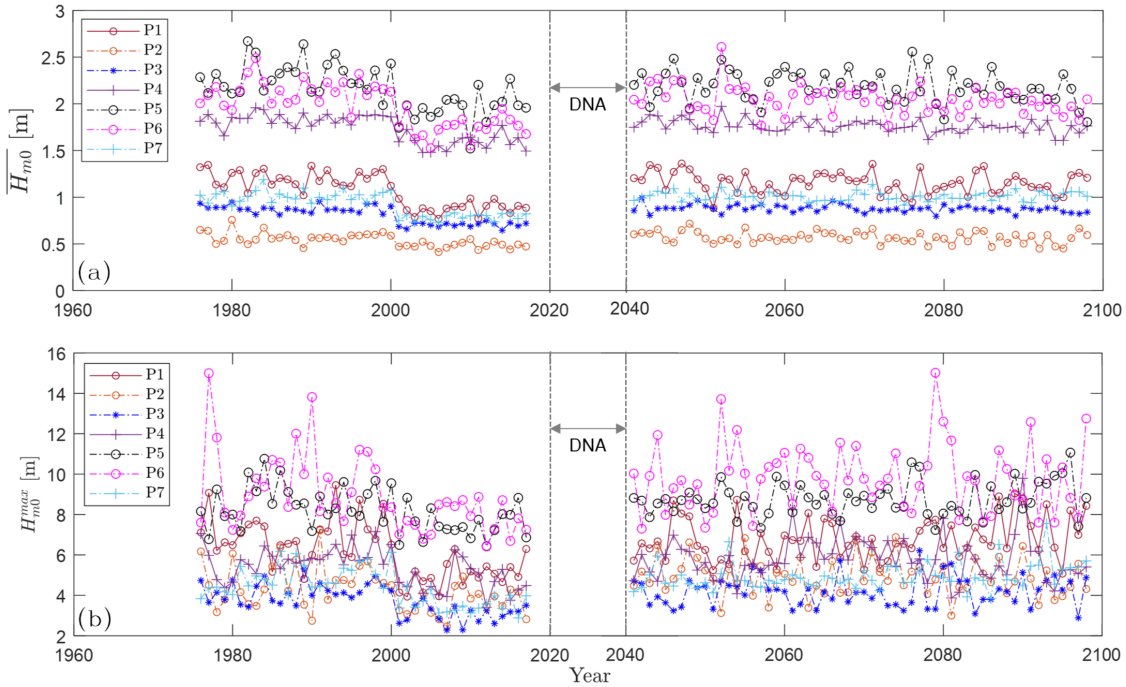

Figure 4. Time series of annual mean and maximum significant wave height $\overline{H_{m0}}$ (**a**) and H_{m0}^{max} (**b**) for the reference locations P1-P7 identified in Figure 3. DNA: Data Not Available in CDS dataset (for the period 2017–2040).

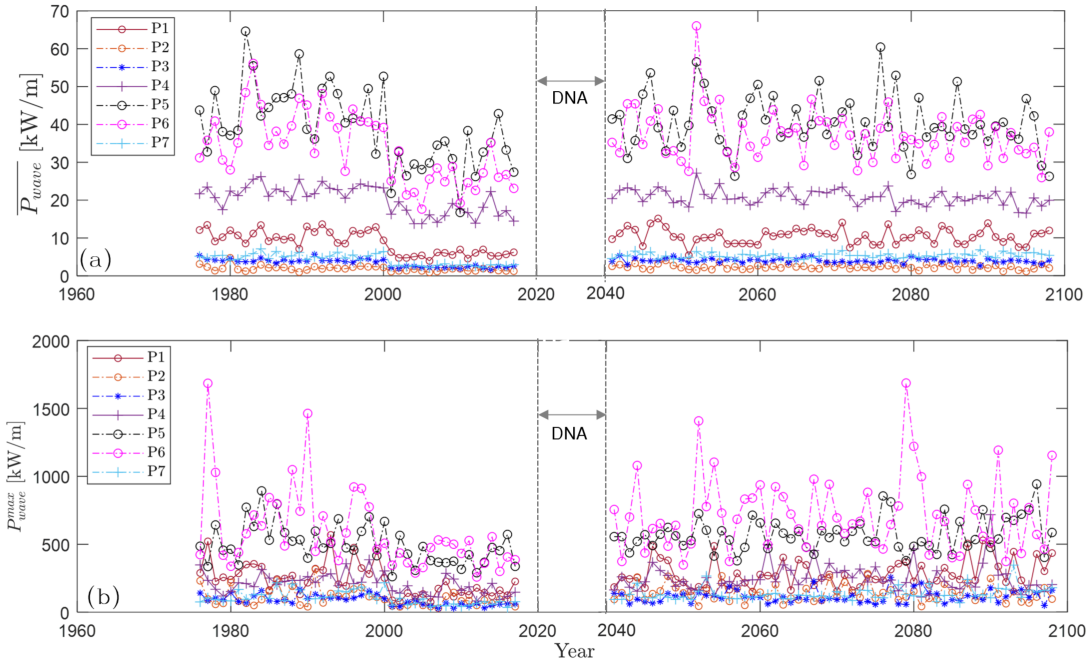

Figure 5. As in Figure 4, but for the mean and maximum wave power $\overline{P_{wave}}$ (**a**) and P_{wave}^{max} (**b**).

P4 is located off the coast of Morocco, and exhibits a significant decreasing trend in $\overline{P_{wave}}$, while no trends are detected in the maximum values P_{wave}^{max}. Conversely, for P5 and P6, located in the North Atlantic, the trend is not significant for the annual average wave power, while it is significant (and increasing) for the maximum values. P7, in the central area of the Baltic Basin, showed a significant trend towards an increase for both $\overline{P_{wave}}$ and P_{wave}^{max}. For locations in the Mediterranean Sea (P1–P3) and in the Baltic Sea (P7), $\overline{H_{m0}}$ ranges between 0.5 and 1.4 m (with $\overline{P_{wave}}$ from 2 to 15 kW/m), while in the Atlantic locations (P4–P6), it ranges between 1.6 and 2.7 m (with $\overline{P_{wave}}$ from 20 to 65 kW/m). In P1–P3 and P7, H_{m0}^{max} varies between 2 and 8 m (with maximum annual wave power of 100–500 kW/m), while in P4-P6, it reaches values of 15 m, with maximum power P_{wave}^{max} up to 1750 kW/m.

3.2. Present and Future Wave Energy Exploitability

With the aim of investigating the intra-annual stability of the wave energy resource and its possible future variation, the monthly variability is examined through the MVI. At the Mediterranean basin scale, the highest MVI in the present scenario is found in the south of Italy, the Gulf of Sirte, and the Levantine Sea area (Figure 6a), where MVI_P is up to 1.5. The lowest MVI_P values, which are an index of the greater stability of the wave energy availability in the short-term perspective, are in the Alboran Sea area and along the Mediterranean coast of Spain, France, and North Italy (Ligurian Sea), where $0.5 \leq MVI_P \leq 1$. In both the projected future scenarios F1 (2040–2070) and F2 (period 2070–2100), an increase in the monthly variability in the wave energy is foreseen, particularly along the northern coast of the Mediterranean Basin (Figure 6b,c). The relative increase between the present and the future MVI, ΔMVI, reaches values of up to 100% in the Ligurian Sea and along the coasts of Greece, in both scenarios F1 and F2.

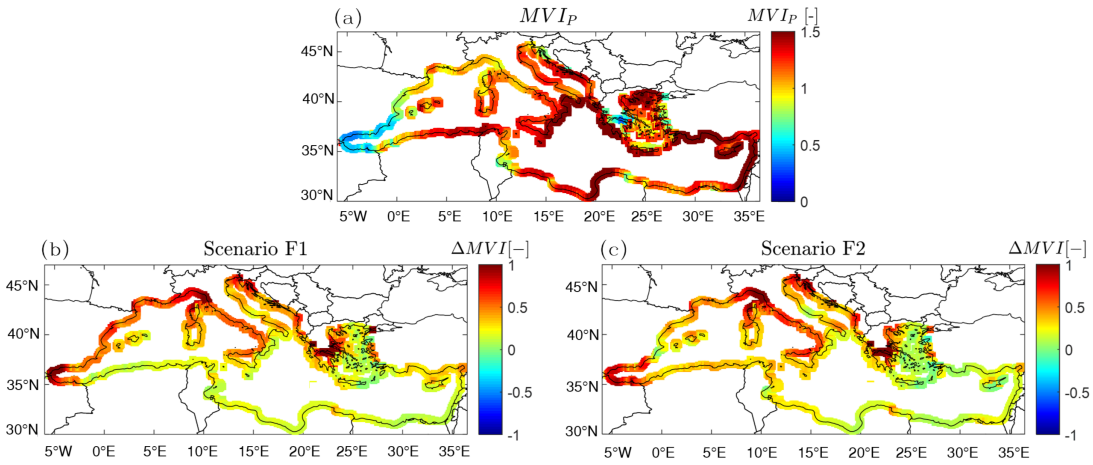

Figure 6. Monthly Variation Index (MVI) in the present wave climate scenario (**a**) and relative variation in the future scenarios F1 (**b**) and F2 (**c**) under RCP8.5 of IPCC for the Mediterranean Basin.

As for the WEDI, in the present scenario, values are lower than 0.05 over the whole Mediterranean basin, with slightly higher values (i.e., denoting more favorable conditions for the installation of WECs) in the north-west areas of the Basin (Figure 7a). After a transition phase characterized by alternating areas with an increase or decrease of the WEDI in the nearest future (scenario F1, Figure 7b), scenario F2 seems to be characterized by a prevalence of decreasing WEDIs (Figure 7c), with $\Delta WEDI$ of up to −25%.

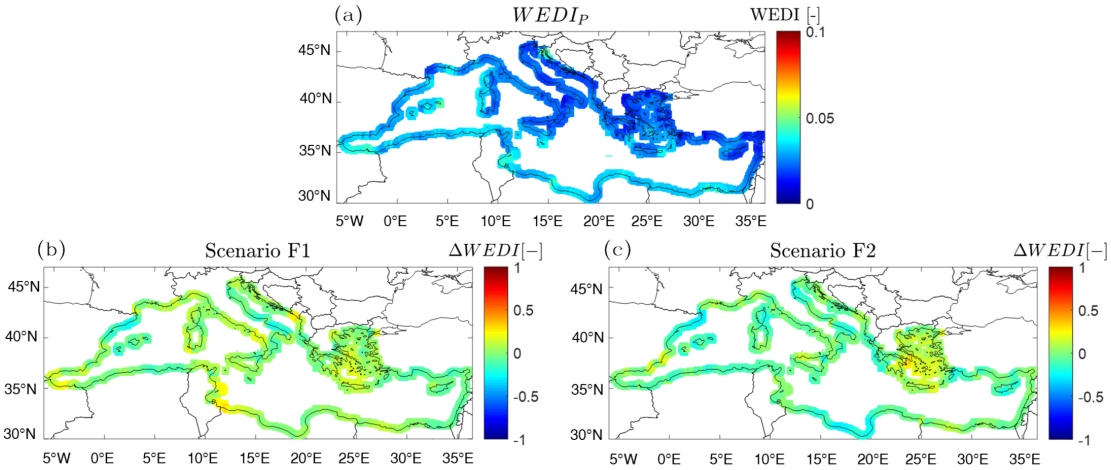

Figure 7. Wave Energy Development Index (WEDI) in the present wave climate scenario (**a**) and relative variation in the future scenarios F1 (**b**) and F2 (**c**) under RCP8.5 of IPCC for the Mediterranean Basin.

For the Atlantic Coasts of Western Sahara, Morocco, and Portugal (Figure 8), the present MVI_P has a maximum of up to 1.8 (in the Azores Archipelago) and values around 1.5 along the coasts of Portugal. Lower values (between 1 and 0.5) are found for latitudes $\leq$30° N. A moderate increase in the monthly variability in the wave energy resource is expected in the future scenarios F1 and F2 (Figure 8b,c), with ΔMVI up to 30%. In the same area, the present $WEDI_P$ reaches values of up to 0.13 along the coast of Western Sahara (Figure 8d), and minimum values of around 0.025 in the South of Portugal and Spain, close to the Strait of Gibraltar. Along the coasts of Portugal and Morocco, the WEDI could decrease by up to 20% in the future scenarios, while an increase of up to 25% is projected for the Western Sahara areas. It is worth stressing that, due to the relatively low MVI and high

WEDI, as well as the limited variation foreseen for future scenarios, the Western Sahara coasts seem to be particularly suitable for WEC exploitation.

Relatively high values of the MVI, varying between 1.4 and 1.5, are found in most of the western coasts of France and the United Kingdom (Figure 9a), with a relevant (i.e., between 30 and 70%) expected further increase in the future scenarios (Figure 9b,c). In this area, $WEDI_P$ higher than 0.07 are found on the Western coasts of France, Ireland, and the UK, while lower $WEDI_P$ (0.02–0.04) characterize the Irish Sea and the English Channel area (Figure 9b,c). The expected relative variation of the WEDI in the future is limited to a range of ±15%.

In the North, Baltic, and Norwegian Seas (Figure 10) the maximum MVI is around 1.5, with the highest values located along the coasts of Norway. In the Baltic Sea, the MVI is more limited, i.e., between 0.7 and 1.2. However, the long-term variation in the wave conditions related to climate change may induce an increase in the monthly variability in the range of 25–75% in the projected scenario F1 (period 2040–2070), further increasing to values close to 100% when extending the time frame to 2100. Furthermore, in this area, the present $WEDI_P$ is mainly in the range 0–0.05, with an expected moderate increase (of the order of 10–20%) over most of the Baltic area in both the future scenarios F1 and F2 (Figure 10e,f). An increase in the intra-annual variability in the Northeast Atlantic by the end of the 21st Century has also been foreseen by Aarnes et al. [57].

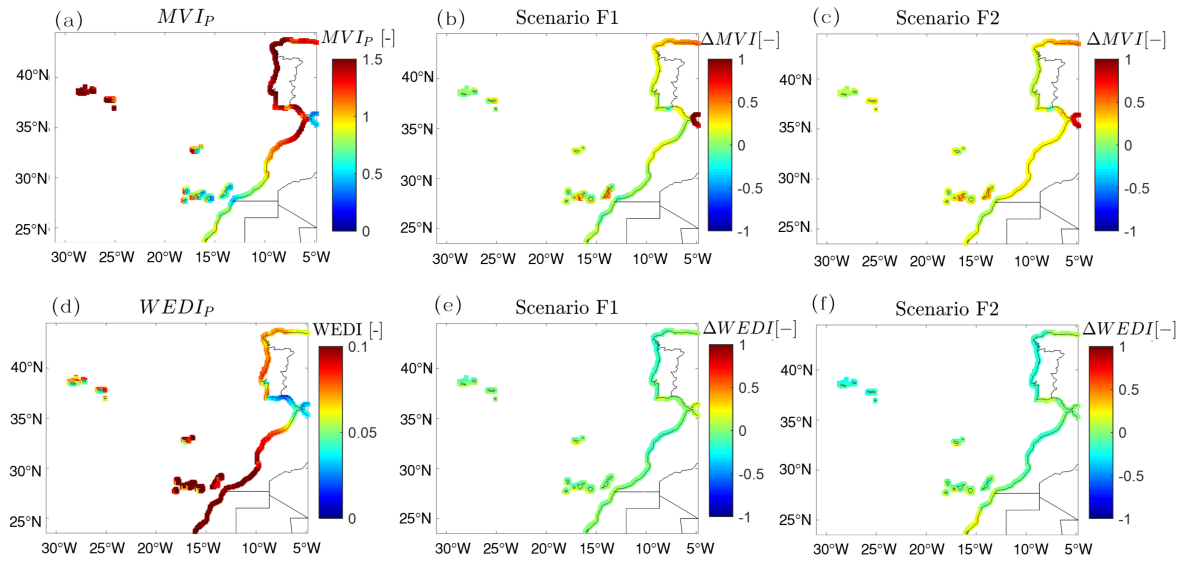

Figure 8. Monthly Variation Index (MVI) and Wave Energy Development Index (WEDI) in the present wave climate scenario (**a**,**d**) and relative variation in the future scenarios F1 (**b**,**e**) and F2 (**c**,**f**) under RCP8.5 of ICCP for the Atlantic coasts of Western Sahara, Morocco, and Portugal.

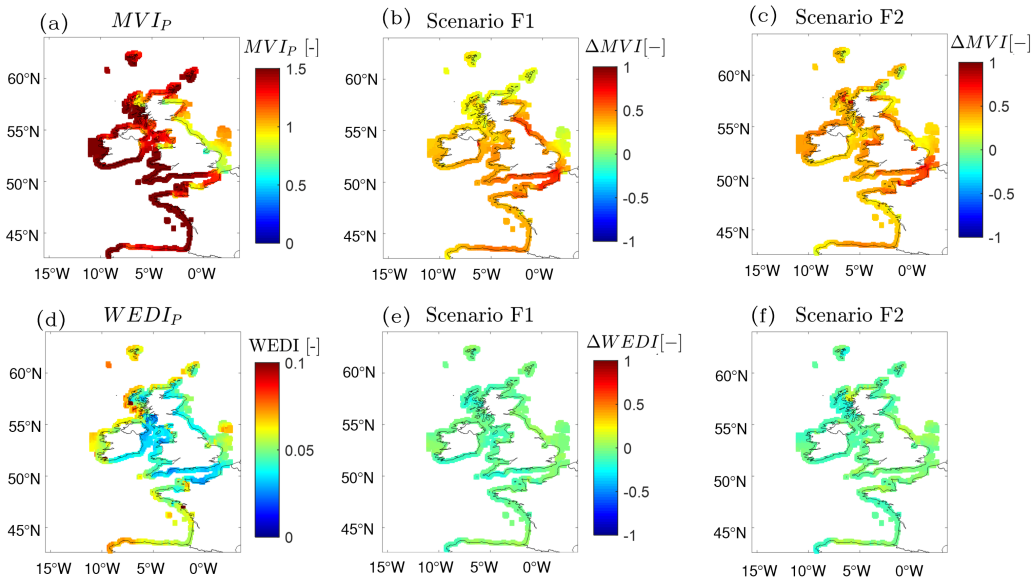

Figure 9. As in Figure 8, but for the Atlantic coasts of Spain, France, and the United Kingdom.

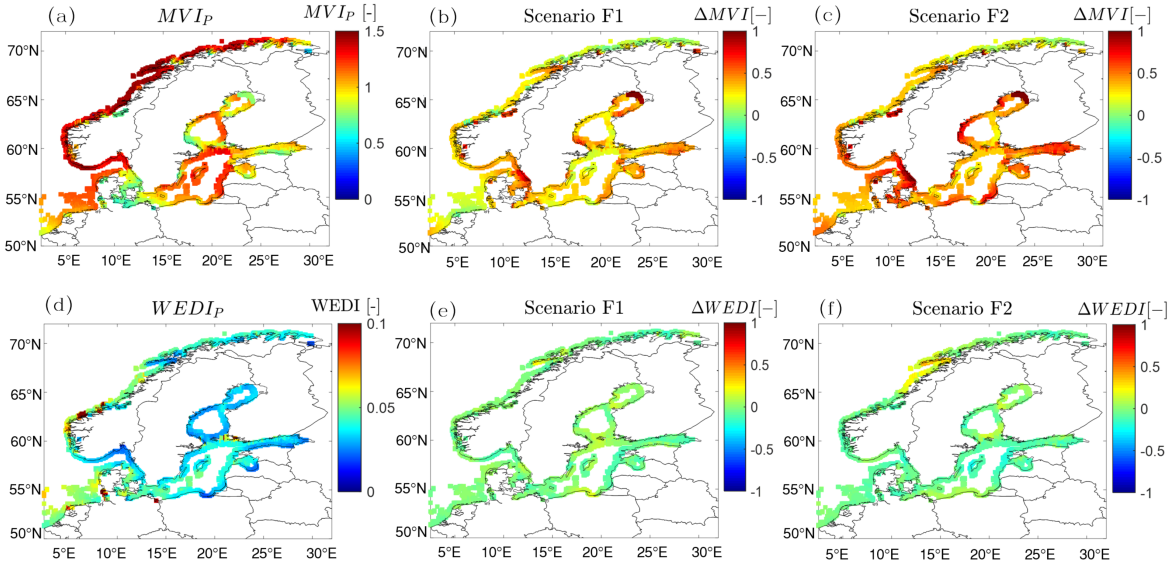

Figure 10. As in Figure 8, but for the coasts of the North, Baltic, and Norwegian Seas.

3.3. Present and Future WEC Performance

The Annual Energy Production (AEP) of the selected set of WECs, with performance characterized in terms of PM as detailed in Section 2.3, in the present wave climate and in the future scenarios based on projected data for RCP8.5 is presented in this section.

For the AquaBuoy device (Figures 11 and 12), the present AEP varies between a maximum of around 800 MWh/year for installations along the north-west coasts of Ireland and the UK, to a minimum below 10 MWh/year. In the Mediterranean Basin, the highest AEP is found along the West Sardinia coast and the coasts of Algeria and Tunisia (≈150 MWh/year, Figure 11a).

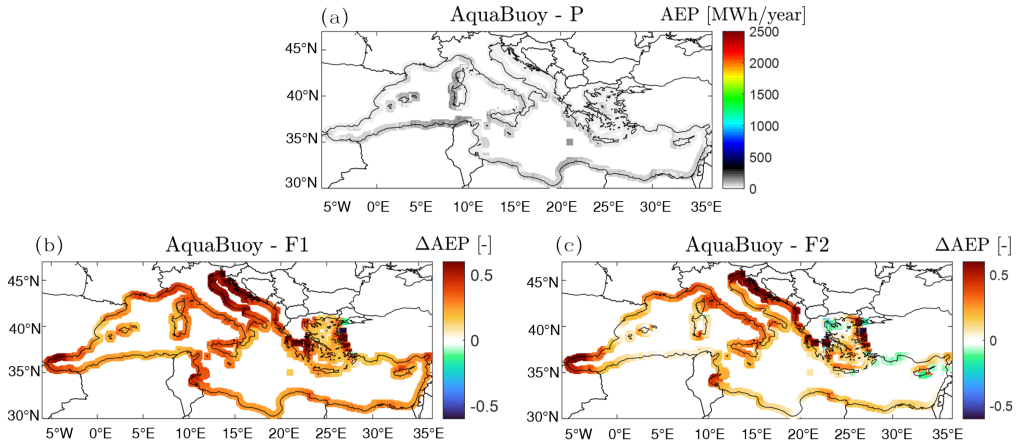

Figure 11. Annual Energy Production (AEP) of the AquaBuoy WEC in the present wave climate (**a**) and relative variation in scenarios F1 (**b**) and F2 (**c**) in the Mediterranean basin.

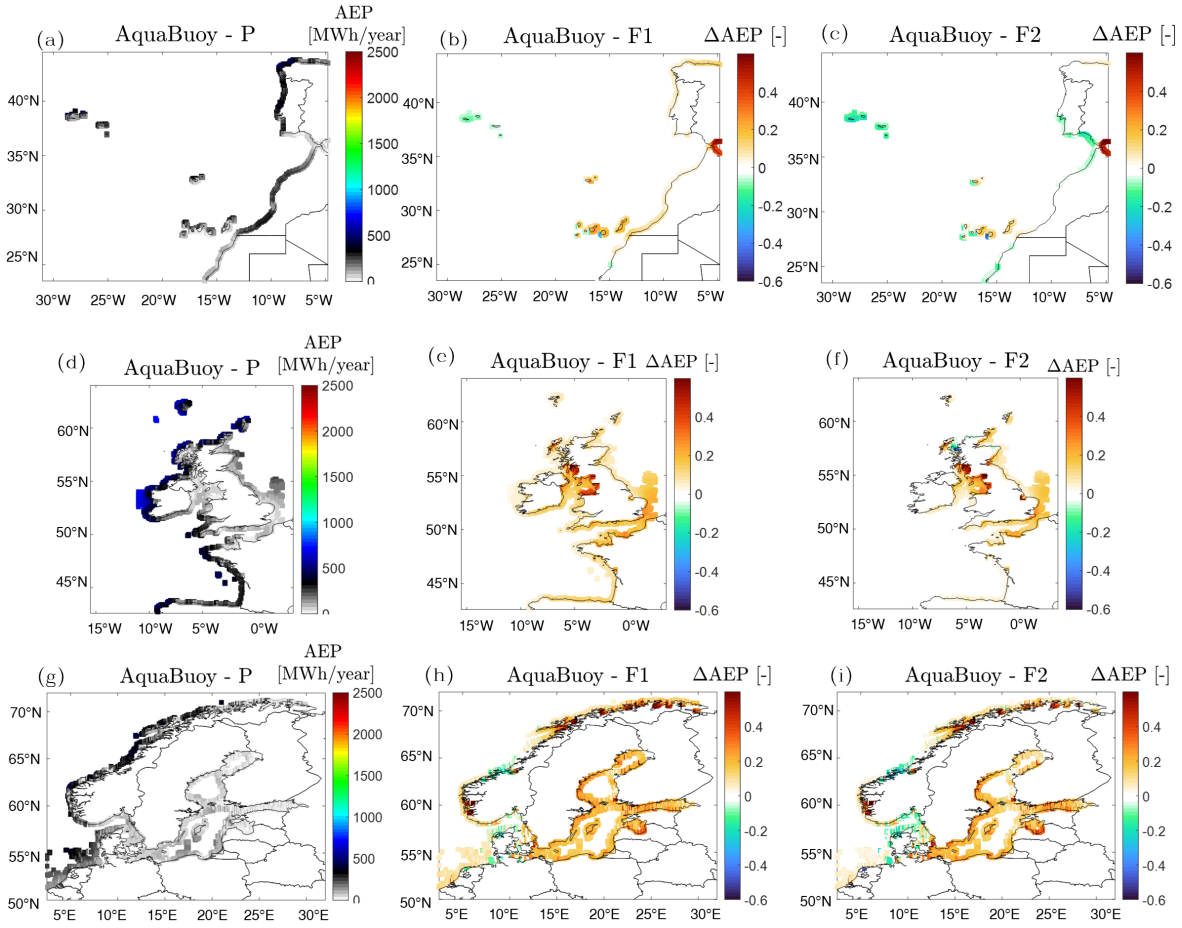

Figure 12. Annual Energy Production (AEP) of the AquaBuoy WEC in the present (**a**,**d**,**g**) wave climate and relative variation in the future F1 (**b**,**e**,**h**) and F2 (**c**,**f**,**i**) scenarios for the North African and European Oceanic coastal waters.

Although the energy production of the device is considerably lower in the Mediterranean, this geographical area will experience greater relative increases in energy production in future scenarios: for the period 2040–2070 (Figure 11b), a relative increase in the AEP of around 50% is expected in the Adriatic Sea, while for most of the north Mediterranean Basin, the increase ranges between 30 and 40%.

A general tendency towards an increase in the AEP of the AquaBuoy device in the future scenarios is observed also for most of the North African and European Atlantic coasts, as well as in the Baltic basin (Figure 12), even if such an increase is more limited in magnitude compared to that of the Mediterranean (i.e., with an average value of around 20%). A moderate relative decrease ($\approx -15\%$) in the projected AEP is observed in the South of Portugal and Spain, around the Gibraltar Strait area, for the distant future scenario F2 (Figure 12c) and around the Azores Archipelago and Denmark in both scenarios F1 and F2.

Overall, areas characterized by the greater AEP for the AquaBuoy are the same for the other devices considered in this study, being strongly related to geographical locations in which the wave resource availability is higher. Results for the AWS are reported in Figures 13 and 14, for the Langlee in Figures 15 and 16, for the OWC in Figures 17 and 18, and for the OEbuoy in Figures 19 and 20. In the Mediterranean Basin, maximum AEP values along Western Sardinia, Corsica, Algeria, and Tunisia reach a value of around 900 MWh/year for the AWS device (Figure 13a), around 790 MWh/year for the Langlee WEC (Figure 15a), 330 MWh/year for the fixed OWC (Figure 17a), and 770 MWh/year for the OEbuoy (Figure 19a). For the North African and European Atlantic coasts, the highest AEP values in the present wave scenario are found in western Ireland, northern UK, the north of Spain, and west of France, with values of up to 2500 MWh/year for the AWS device (Figure 14a,d), 1500 MWh/year for the Langlee WEC (Figure 16d), around 1000 MWh/year for the fixed OWC (Figure 18d), and around 2500 MWh/year for the OEbuoy (Figure 20d).

The general trends in the relative variation in the AEP in the future scenarios observed for the AquaBuoy device are also confirmed for the other WECs: The overall Mediterranean basin is characterized by an increase in the AEP, which is particularly evident in the nearest future scenario F1 and less strong for F2. The energy production of the AquaBuoy, OEbuoy, and AWS devices will have higher relative increases compared to those of the other devices, with an average value over the whole Mediterranean Basin of around 30% (to be compared with an average value of 20% for the fixed OWC and Langlee). For the fixed OWC and the Langlee device, the future relative variation in the energy production is negligible (i.e., up to $\pm 10\%$) for the coasts of Western Sahara, Morocco, and Portugal (Figures 16b,c and 18b,c) and the Atlantic coasts of Spain, France, and the United Kingdom (Figures 16e,f and 18e,f). The lower variation in the energy production of the fixed OWC and Langlee in the future wave climates in these areas may be explained by considering that based on the available PM, such devices have the maximum energy extraction capability for relatively short ($T_{m-1,0} \leq 8$ s), i.e., in a portion of the scatter matrix that remains relatively unchanged in the future scenarios F1 and F2 in the aforementioned geographical locations. All devices, instead, show a quite remarkable increase in the AEP in the Baltic Basin (with values of ΔAEP in the range 15–30%), with the OWC and the Langlee still showing the smallest variations.

It is worth noting that, for all the devices and the majority of the analyzed locations, the relative increases in the AEP in the projected wave scenario are stronger for the near future F1 (2040–2070) than for the distant future F2 (2070–2100). This is a direct consequence of the greater wave energy availability in the scatter matrices of scenario F1 compared to scenario F2, especially corresponding to couples of H_m and $T_{m-1,0}$ that can be efficiently exploited by the considered WECs. This stronger variation in the wave energy resource in the near future compared to the distant future is also confirmed at the scale of the Mediterranean Basin in the work of Loarca et al. [17].

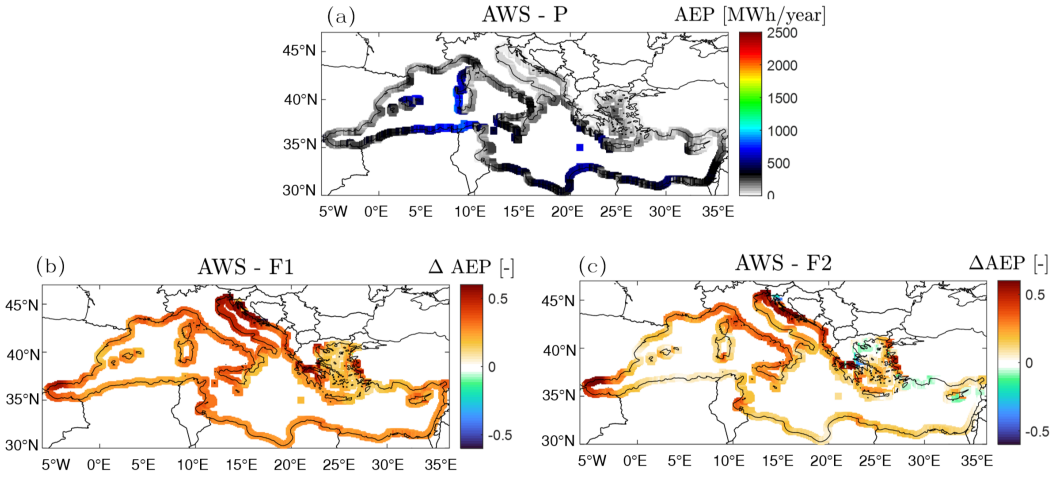

Figure 13. Annual Energy Production (AEP) of the AWS WEC in the present wave climate (**a**) and relative variation in scenarios F1 (**b**) and F2 (**c**) in the Mediterranean basin.

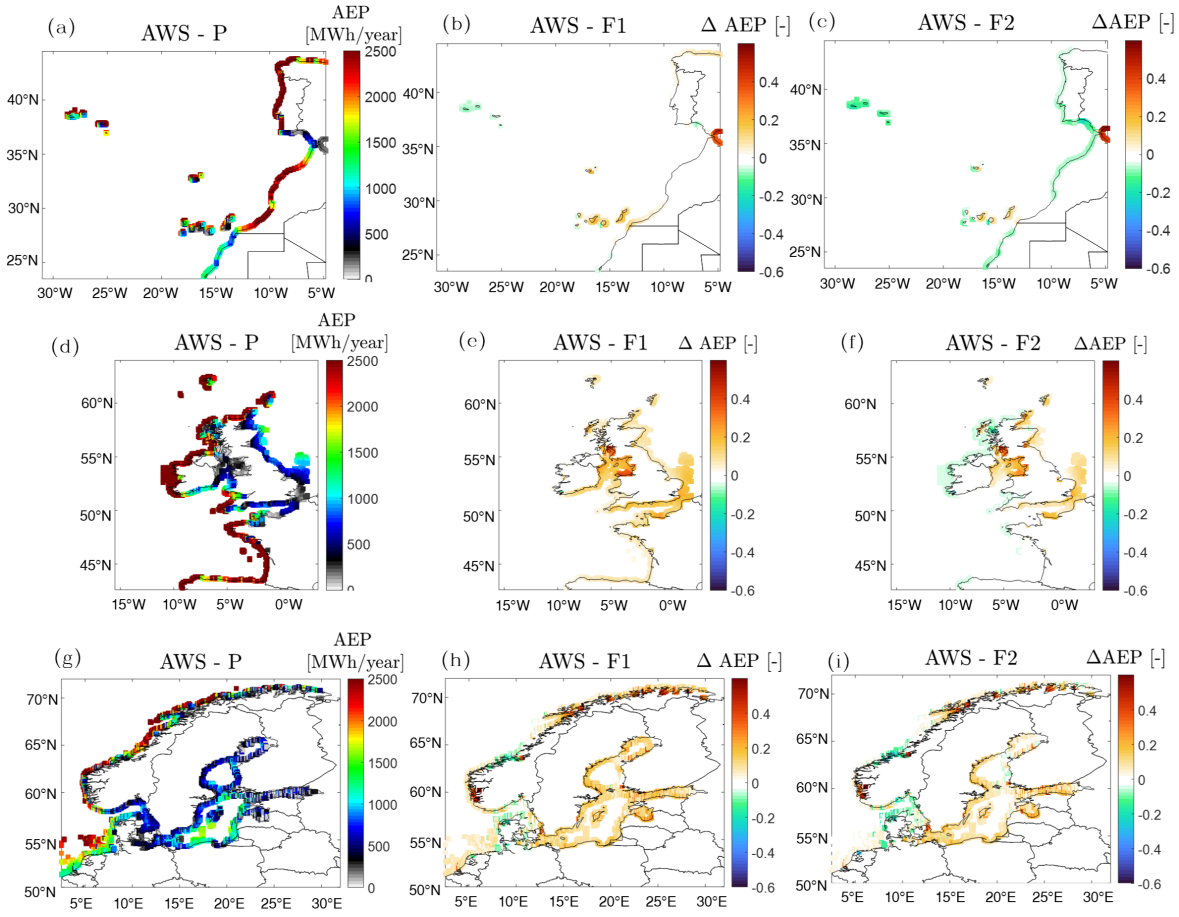

Figure 14. Annual Energy Production (AEP) of the AWS WEC in the present (**a**,**d**,**g**) wave climate and relative variation in the future F1 (**b**,**e**,**h**) and F2 (**c**,**f**,**i**) scenarios for the North African and European Oceanic coastal waters.

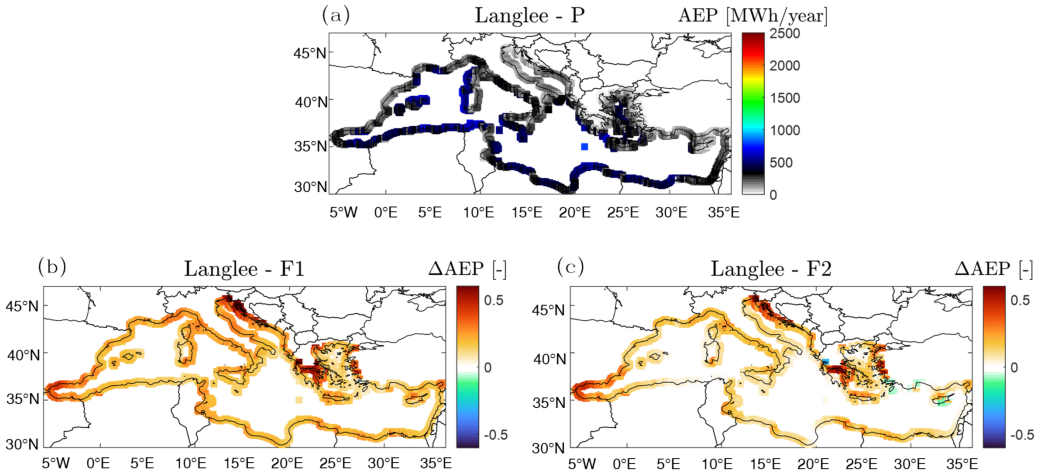

Figure 15. Annual Energy Production (AEP) of the Langlee WEC in the present wave climate (**a**) and relative variation in scenarios F1 (**b**) and F2 (**c**) in the Mediterranean basin.

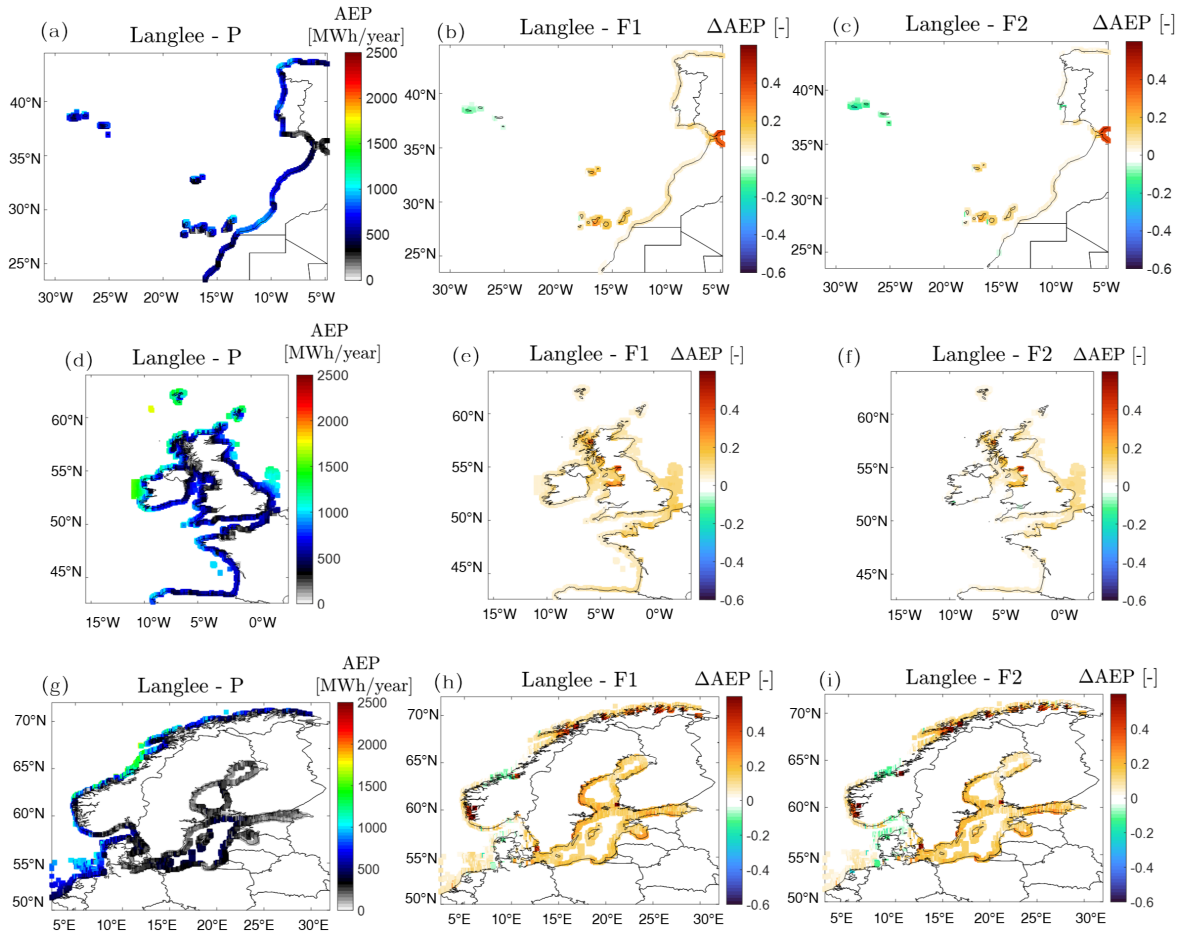

Figure 16. Annual Energy Production (AEP) of the Langlee WEC in the present (**a**,**d**,**g**) wave climate and relative variation in the future F1 (**b**,**e**,**h**) and F2 (**c**,**f**,**i**) scenarios for the North African and European Oceanic coastal waters.

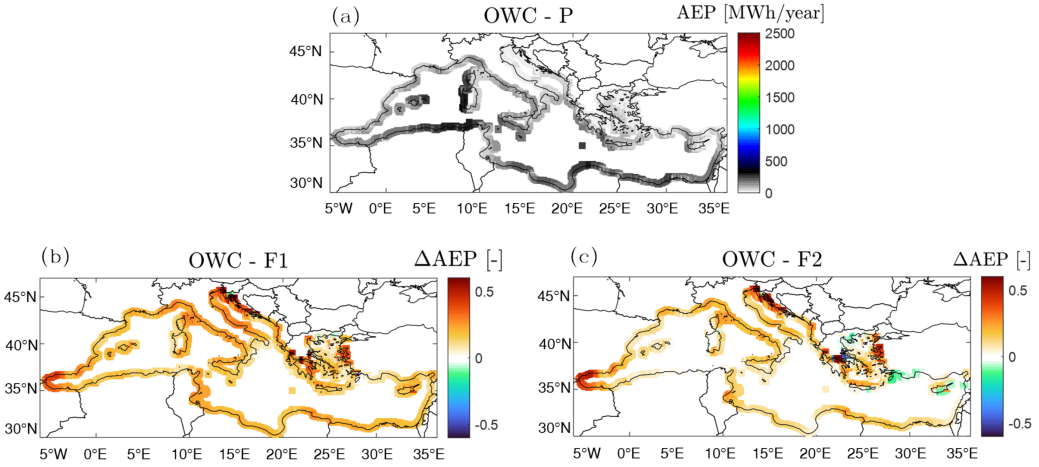

Figure 17. Annual Energy Production (AEP) of the OWC WEC in the present wave climate (**a**) and relative variation in scenarios F1 (**b**) and F2 (**c**) in the Mediterranean basin.

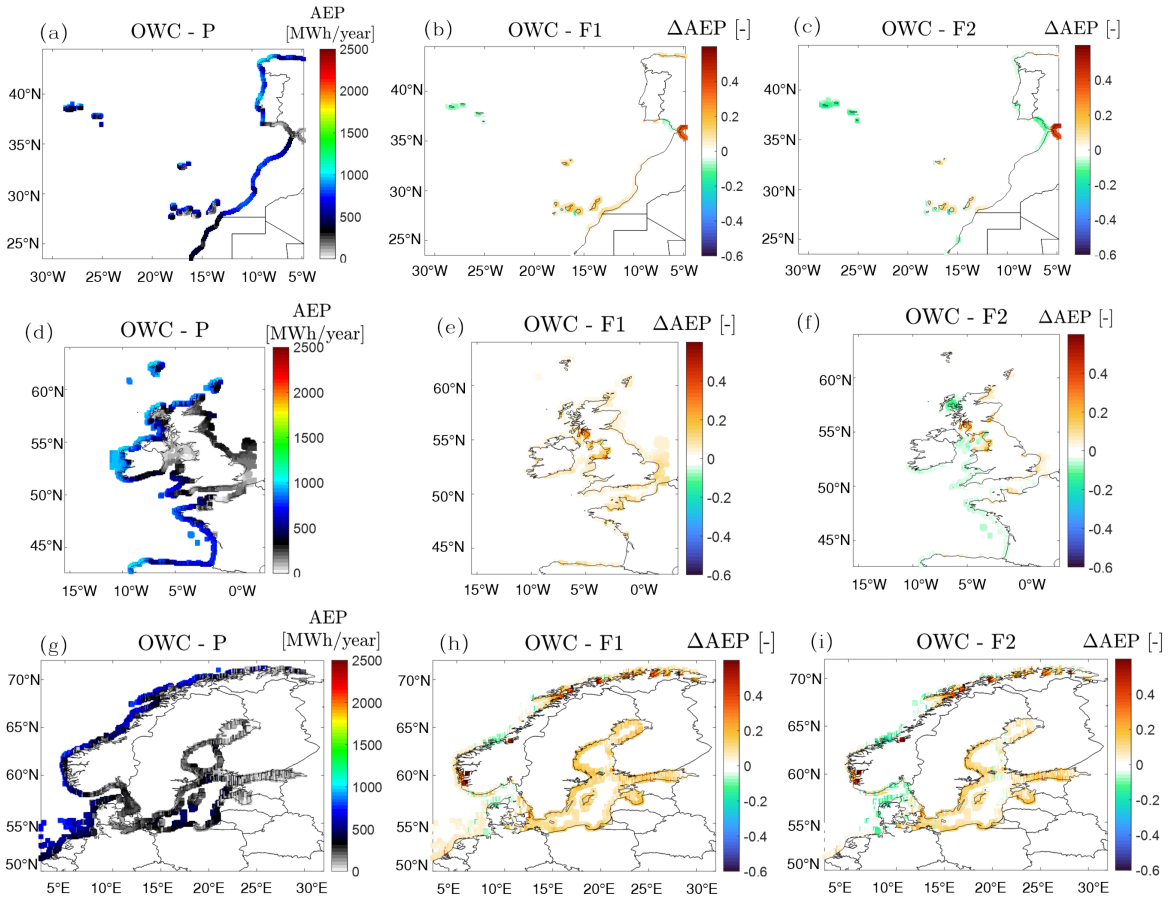

Figure 18. Annual Energy Production (AEP) of the OWC WEC in the present (**a**,**d**,**g**) wave climate and relative variation in the future F1 (**b**,**e**,**h**) and F2 (**c**,**f**,**i**) scenarios for the North African and European Oceanic coastal waters.

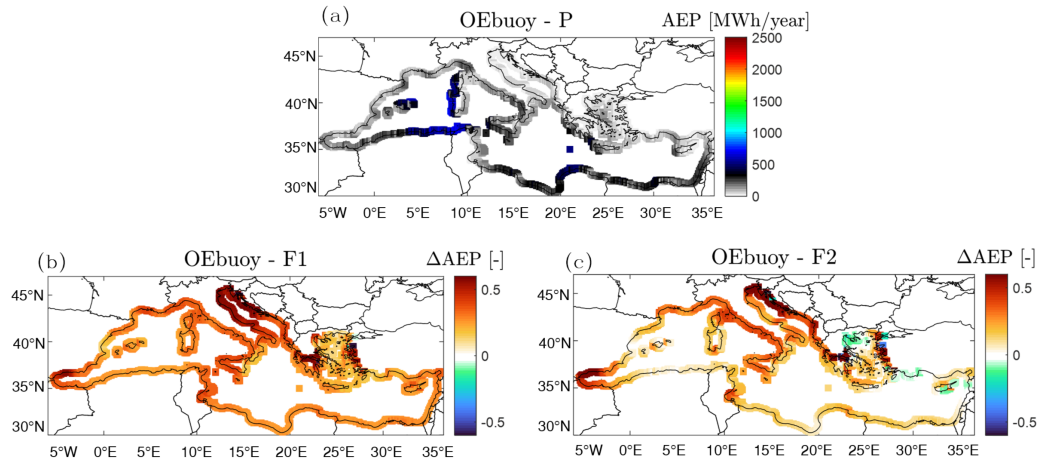

Figure 19. Annual Energy Production (AEP) of the OEbuoy WEC in the present wave climate (**a**) and relative variation in scenarios F1 (**b**) and F2 (**c**) in the Mediterranean basin.

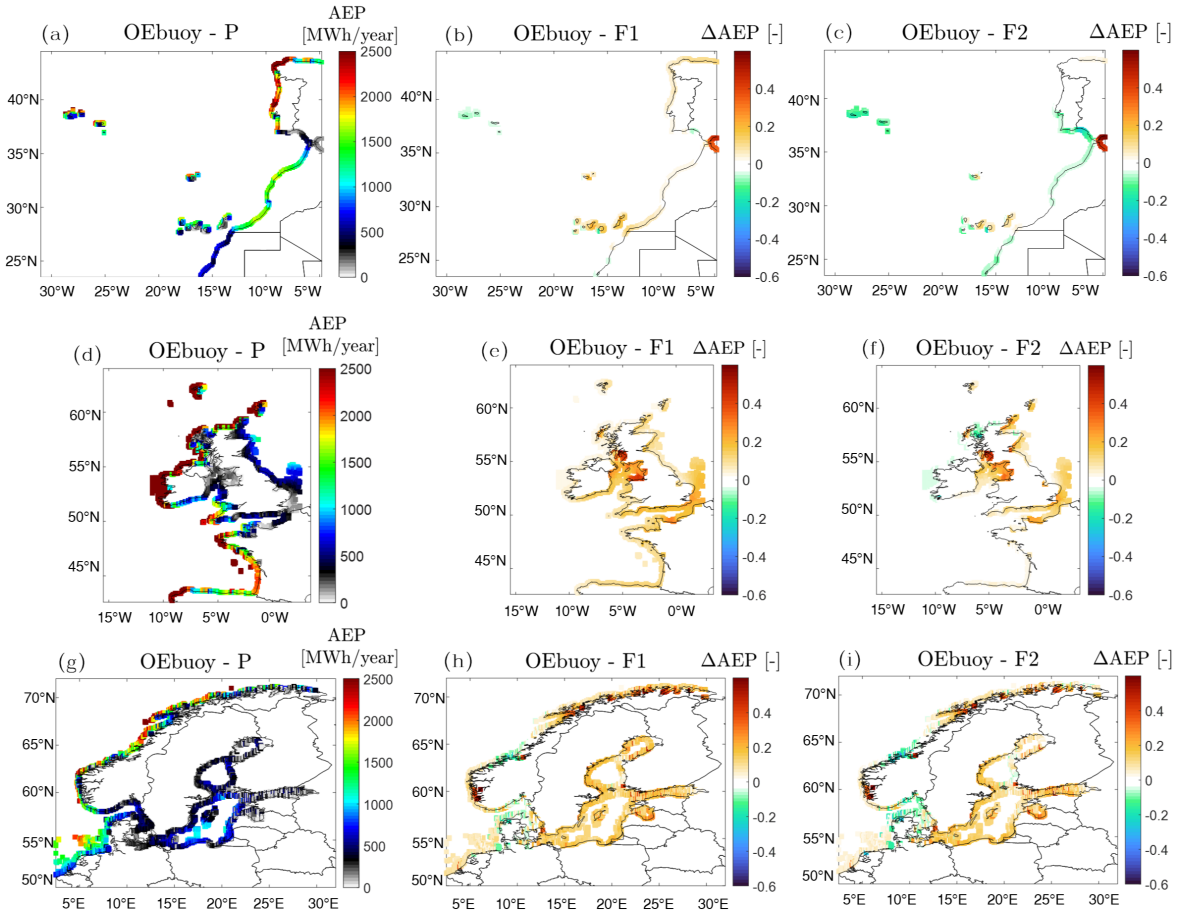

Figure 20. Annual Energy Production (AEP) of the OEbuoy WEC in the present (**a**,**d**,**g**) wave climate and relative variation in the future F1 (**b**,**e**,**h**) and F2 (**c**,**f**,**i**) scenarios for the North African and European Oceanic coastal waters.

In Table 2, we explicitly reported the AEP of the selected WECs in the locations P1–P7 (introduced in Figure 3) to allow for a clearer visualization of the results.

Table 2. Annual Energy Production AEP [MWh/year] of the selected WECs in locations P1–P7 for the present scenario P, near-future scenario F1 and distant future scenario F2.

Device-Scenario	P1	P2	P3	P4	P5	P6	P7
AquaB-P	130	19	37	221	377	329	72
AquaB-F1	159	26	47	230	393	352	90
AquaB-F2	146	25	42	216	366	329	92
AWS-P	659	110	257	2314	3578	3172	920
AWS-F1	815	145	326	2331	3581	3293	1046
AWS-F2	761	139	295	2181	3369	3094	1040
Langlee-P	651	168	272	697	840	760	241
Langlee-F1	736	199	334	2331	893	808	287
Langlee-F2	688	186	316	2181	852	779	293
OWC-P	262	63	152	744	852	751	290
OWC-F1	289	69	184	772	871	758	337
OWC-F2	265	66	168	733	828	713	333
OEbuoy-P	530	79	190	1399	2601	2238	530
OEbuoy-F1	667	108	238	1430	2656	2427	628
OEbuoy-F2	631	104	213	1330	2514	2270	634

4. Discussion

A sound understanding of the long-term trends in the variation in sea waves is crucial for many applications in the field of maritime engineering, from studies related to coastal flooding risk and development of adaptation strategies to the planning and design of WEC installations. Accurate quantification of these trends is still ambitious from a technical and scientific point of view, and inherently affected by inevitable limitations induced by both the accuracy of numerical wave models and the uncertainty in climate-forcing projections. The different sources of uncertainty in such kind of quantification have been discussed by Lobeto et al. [58], who specifically focused on assessing the uncertainty related to the wave modeling and highlighted that divergences in the projected change may rise due to the use of different numerical models or different model parametrizations, particularly for the projected changes in the wave period. As aforementioned, the present study is conducted using data provided by the Copernicus CDS [31], and as such, the uncertainties in this database propagate to the results of this work.

This work highlighted a diffused divergence in the trends for annual mean values of wave power $\overline{P_{wave}}$ and maxima annual power P_{wave}^{max}. Areas where trends are significant also differ between mean and maximum conditions. A similar divergence was also previously found in [17] for several oceanic areas. Despite the consistency of results with previous studies and the aforementioned inherent uncertainties of modeling the future wave climate, it is important to also underline that locations identified as statistically significant can be remarkably different based on the statistical method adopted, as discussed in [8]. The data presented in this work may provide insight into the projected trends in the wave energy potentials at a European level. However, based on the current state of the art on the identification of trends in wave data, both at the regional and global scale, there is a well-recognized need to further improve the reliability of the results by more precise quantification of the uncertainty related to the numerical models used to produce the data (as highlighted by De Leo et al. [23], Liu et al. [9], and Lobeto et al. [58]). On this aspect, future research is needed to strengthen the consensus in the knowledge of long-term trends, e.g., by adopting approaches similar to that proposed in Loarca et al. [59], where results are bias-corrected and averaged before assessing the presence of a trend. It is also worth pointing out that the present study, as most of the previous ones, considers integrated wave parameters, while Lobeto et al. [60] suggested that analyzing variations within the directional spectrum could lead to remarkably different conclusions about the

changes in the wave conditions in a given location. Such aspects are out of the scope of the present work.

Concerning the indexes used to characterize wave energy exploitability, this study found, for the present wave climate scenario, values of MVI between 0.5 and 1.8 along the European Coasts, with WEDI always lower than 0.1. As a comparison, for the MVI, in [39], values of 0.5–1 were found for the Southern Indian Ocean, while higher values ($1.5 \leq MVI_P \leq 3.5$) were obtained for the Northern Indian Ocean in the present wave climate. Along the coasts of the South China Sea, the present MVI reaches values of 0.8–1.6 [41]. For the Mediterranean Sea, values of the WEDI found in this study are consistent with those provided in [40,61] (where WEDI values lower than 0.1 were found over the whole Mediterranean Basin, with values of 0.01–0.03 in the Aegean Sea [61]). The energy production in the present wave climate scenario estimated for the selected devices is consistent with previous studies available in the literature, based on hindcast wave data obtained with different numerical models: for an OWC with a 4 m width, an AEP of around 220 MWh/year for an installation in the Biscay Bay was found in [51], while in the same location, the AEP increases to around 2000 MWh/year for an AWS device. For the Mediterranean Sea, values of AEP between 200 and 300 MWh/year near the coasts of Calabria were estimated for the AWS, the Langlee, and the OEbuoy [62], closely matching the estimations in this work. AEP values between 120 and 200 MWh/year were found for the installation of an AquaBuoy device near the island of Crete [61], slightly higher than that found in this work (i.e., up to $\pm$110 MWh/year in the same area). Along the west coast of Sardinia, near Alghero, a maximum AEP for the AquaBuoy of 192 MWh/year was estimated [63], to be compared with a value of 175 MWh/year obtained in this work. The magnitude of the site-specific variation in the performance of WECs when adopting a long-term perspective has also been confirmed by Ulazia et al. [28]. Despite the consistency of the previous results with previous ones, it is worth stressing that the description of the performance of a WEC solely based on the PM approach can be affected by significant limitations in accuracy, as discussed in [64]. Using a PM-based approach can result in an error of up to 20% in the estimation of the AEP of a WEC, compared to computing the power output with more elaborate time-domain approaches. Moreover, the present study does not account for the possible change in wave direction in future wave climate scenarios, nor the effect of wave directionality on WEC performance. Indeed, despite the recognized importance of this parameter, information on wave direction is not disclosed in most of the available PMs of the WECs.

It should also be stressed that in the present work, the energy conversion performance of the WECs has been obtained considering PMs of devices not specifically optimized for the installation in a specific location, since the main objective of the study is the evaluation of relative changes in the present and future scenarios induced by climate change considering as fixed the design characteristics of the WEC, both in terms of geometry and Power Take Off (PTO), and without long-term control systems. On this regard, it is expected that any relevant change in the wave climate would result in a variation in the optimal design of the WEC, which is indeed strongly site-specific and requires a combined optimization of the device geometry and the PTO system (as discussed, e.g., in Simonetti et al., 2016 [65] and 2017 [55]). For the specific case of an OWC device, significant variations in the optimal design parameters in time, for the installation in a given location, were previously discussed by Ulazia et al. [29] (for the period 1979–2018) and Simonetti et al. [22,30] (for the period 1976–2100). Both studies concluded that the differences in optimal geometries considering long-term variations in wave climate reached up to 15% in several installation sites. The geometry and PTO optimization analysis could be extended to other devices in future works, as well as the development of long-term control strategies for WECs. Moreover, this study is not intended to address the profitability of investing in a specific WEC. Indeed, the traditional indexes deployed to evaluate whether a device is more or less advantageous from an economic point of view (e.g., the capacity factor or the levelized cost of energy) are not considered here. Finally, it is worth remarking that the increase in a WEC's annual

energy production obtained in this study in the future scenarios, relative to the present one, is based on a characterization of present wave climate with CDS of Copernicus data'[31], which are, in turn, based on ERA5 winds. ERA5 data were found to underestimate wind conditions in some Mediterranean locations (e.g., in the Aegean Sea [66], or in the Southeastern Mediterranean Basin [67]). Barbariol et al. [12] also confirmed that despite being able to properly reproduce trends and temporal variability in the wave climate, ERA5-based wave hindcasts show a general tendency to underestimate the significant wave height in several Mediterranean basin areas. This partial underestimation of the present wave condition may exacerbate the increase in the AEP expected in several areas of the Mediterranean Basin fo the near future.

5. Conclusions

In this work, an analysis of the possible trends in the variation in future wave power along the 20 m bathymetric contours of the Mediterranean Basin, the Atlantic Ocean off the coasts of North Africa and Europe, and the European coasts of the North, Baltic, and Norwegian Seas is carried out. The data provided by the Climate Data Store of the Copernicus Climate Change Service (CDS) are used, focusing on projections under the RCP8.5 of IPCC, up to the year 2100. When considering annual mean values of the wave power, areas characterized by a significant increasing trend (e.g., the Alboran Sea, the western coasts of South Italy, the Aegean coasts of Croatia, Greece, Albania, and the Baltic Basin) are geographically alternated with areas in which the trend is markedly decreasing. Significant decreasing trends in the annual average wave power are detected for extended areas along the Atlantic coasts of Western Sahara, Morocco, and Portugal and those of Spain, France, and the United Kingdom. Such a decreasing trend has the highest magnitude along the west coast of Ireland. Conversely, the maximum annual power is characterized by a prevalence of increasing trends in most of the considered areas (with a rate of increase of up to 0.6 kW/m per year in the Mediterranean Basin and 1 kW/m per year along the Atlantic coasts of Portugal). The long-term variation in the characteristics of the wave energy resource in climate change scenarios may have implications on the exploitability of the wave energy, which are summarized as follows:

- The intra-annual short-term variability in the wave energy resource, expressed in terms of the Monthly Variability Index MVI, will generally increase for most of the considered areas, both Mediterranean and Atlantic, up to double the current values in some locations;
- The Wave Energy Development Index WEDI, expressing the ratio of the mean annual wave power to the maximum annual wave power (with lower values denoting more severity installation areas from the point of view of the survivability of the device), is foreseen to have a remarkable relative decrease (of up to -25%) in most of the considered locations, especially for the distant future scenario (years 2070–2100). For the near future (2040–2070), the WEDI shows instead a transitory tendency toward an increase in several locations, particularly inside the Mediterranean Basin;
- For all the analyzed WECs, the Mediterranean Basin is characterized by an increase in annual energy production (up to a maximum of 60%, with an average value at the regional scale of around 30%), which is particularly evident for the nearest future scenario (period 2040–2070). Increases in annual energy production are also expected, for the nearest future scenario, for most of the Baltic Sea, the north coast of Spain, France, and around the UK (even if in these areas the relative increase is lower than 30%). The increase in the potential annual energy production is generally lower in the distant future scenario (2070–2100), to the point of reverting to a moderate reduction of the production in some locations.

Overall, this study suggests that the relative increase in the potential energy production of the devices observed for the projected future wave conditions will have to be accompanied by careful assessments regarding the survival of the devices themselves, which will be called upon to face more intense storms in the coming years. Therefore, in the

context of promoting the transition towards cleaner energy sources and increasing the diffusion of WECs, such aspects will necessarily need to be taken into account for an efficient and reliable design, aimed at ensuring the survivability requirements of the devices.

Author Contributions: Conceptualization, I.S. and L.C.; methodology, I.S. and L.C.; formal analysis, I.S.; investigation, I.S. and L.C.; resources, L.C.; data curation, I.S.; writing—original draft preparation, I.S.; writing—review and editing, L.C.; funding acquisition, L.C. All authors have read and agreed to the published version of the manuscript.

Funding: The research contract of I.S. is co-funded by the European Union—PON Research and Innovation 2014–2020 under Article 24, paragraph 3a), of Law No. 240 of 30 December 2010, as amended, and Ministerial Decree No. 1062 of 10 August 2021.

Data Availability Statement: Research Data available upon request.

Conflicts of Interest: The authors declare no conflicts of interest.

References

1. IPCC. *Climate Change 2014: Synthesis Report. Contribution of Working Groups I, II and III to the Fifth Assessment Report of the Intergovernmental Panel on Climate Change*; Technical Report; IPCC: Geneva, Switzerland, 2014.
2. IEA. *Net Zero by 2050: A Roadmap for the Global Energy Sector*; Technical Report; International Energy Agency: Paris, France, 2021.
3. Taveira-Pinto, F.; Rosa-Santos, P.; Fazeres-Ferradosa, T. Marine renewable energy. *Renew. Energy* **2020**, *150*, 1160–1164. [CrossRef]
4. Cagney, D. *2030 Ocean Energy Vision Industry Analysis of Future Deployments, Costs and Supply Chains*; Technical Report; Ocean Energy Europe: Brussels, Belgium, 2020.
5. Reguero, B.G.; Losada, I.J.; Méndez, F.J. A recent increase in global wave power as a consequence of oceanic warming. *Nat. Commun.* **2019**, *10*, 205. [CrossRef] [PubMed]
6. Sharmar, V.D.; Markina, M.Y.; Gulev, S.K. Global Ocean Wind-Wave Model Hindcasts Forced by Different Reanalyzes: A Comparative Assessment. *J. Geophys. Res. Ocean.* **2021**, *126*, e2020JC016710. [CrossRef]
7. Erikson, L.; Morim, J.; Hemer, M.; Young, I.; Wang, X.L.; Mentaschi, L.; Mori, N.; Semedo, A.; Stopa, J.; Grigorieva, V.; et al. Global ocean wave fields show consistent regional trends between 1980 and 2014 in a multi-product ensemble. *Commun. Earth Environ.* **2022**, *3*, 320. [CrossRef]
8. Casas-Prat, M.; Wang, X.L.; Mori, N.; Feng, Y.; Chan, R.; Shimura, T. Effects of Internal Climate Variability on Historical Ocean Wave Height Trend Assessment. *Front. Mar. Sci.* **2022**, *9*, 847017. [CrossRef]
9. Liu, Q.; Young, I.R.; Zieger, S.; Ribal, A.; Long, S.M.; Dong, X.; Song, Z.; Guan, C.; Babanin, A.V. On global wave height climatology and trends from multiplatform altimeter measurements and wave hindcast. *Ocean Model.* **2023**, *186*, 102264. [CrossRef]
10. Liu, J.; Li, R.; Li, S.; Meucci, A.; Young, I.R. Increasing wave power due to global climate change and intensification of Antarctic Oscillation. *Appl. Energy* **2024**, *358*, 122572. [CrossRef]
11. De Leo, F.; De Leo, A.; Besio, G.; Briganti, R. Detection and quantification of trends in time series of significant wave heights: An application in the Mediterranean Sea. *Ocean Eng.* **2020**, *202*, 107155. [CrossRef]
12. Barbariol, F.; Davison, S.; Falcieri, F.M.; Ferretti, R.; Ricchi, A.; Sclavo, M.; Benetazzo, A. Wind Waves in the Mediterranean Sea: An ERA5 Reanalysis Wind-Based Climatology. *Front. Mar. Sci.* **2021**, *8*, 760614. [CrossRef]
13. Amarouche, K.; Bingölbali, B.; Akpinar, A. New wind-wave climate records in the Western Mediterranean Sea. *Clim. Dyn.* **2022**, *58*, 1899–1922. [CrossRef]
14. Elshinnawy, A.I.; Antolínez, J.A. A changing wave climate in the Mediterranean Sea during 58-years using UERRA-MESCAN-SURFEX high-resolution wind fields. *Ocean Eng.* **2023**, *271*, 113689. [CrossRef]
15. Mel, R.A.; Lo Feudo, T.; Miceli, M.; Sinopoli, S.; Maiolo, M. Robustness and uncertainties in global multivariate wind-wave climate projections. *Nat. Clim. Chang.* **2019**, *9*, 711–718. [CrossRef]
16. Meucci, A.; Young, I.R.; Hemer, M.; Kirezci, E.; Ranasinghe, R. Projected 21st century changes in extreme wind-wave events. *Sci. Adv.* **2020**, *6*, eaaz7295. [CrossRef]
17. Lobeto, H.; Menendez, M.; Losada, I.J. Future behavior of wind wave extremes due to climate change. *Sci. Rep.* **2021**, *11*, 7869. [CrossRef] [PubMed]
18. Bernardino, M.; Gonçalves, M.; Campos, R.; Guedes Soares, C. Extremes and variability of wind and waves across the oceans until the end of the 21st century. *Ocean Eng.* **2023**, *275*, 114081. [CrossRef]
19. Meucci, A.; Young, I.R.; Hemer, M.; Trenham, C.; Watterson, I.G. 140 Years of Global Ocean Wind-Wave Climate Derived from CMIP6 ACCESS-CM2 and EC-Earth3 GCMs: Global Trends, Regional Changes, and Future Projections. *J. Clim.* **2023**, *36*, 1605–1631. [CrossRef]
20. Leo, F.D.; Besio, G.; Mentaschi, L. Trends and variability of ocean waves under RCP8.5 emission scenario in the Mediterranean Sea. *Ocean Dyn.* **2021**, *71*, 97–117. [CrossRef]
21. Lira-Loarca, A.; Ferrari, F.; Mazzino, A.; Besio, G. Future wind and wave energy resources and exploitability in the Mediterranean Sea by 2100. *Appl. Energy* **2021**, *302*, 117492. [CrossRef]

22. Simonetti, I.; Cappietti, L. Mediterranean coastal wave-climate long-term trend in climate change scenarios and effects on the optimal sizing of OWC wave energy converters. *Coast. Eng.* **2023**, *179*, 104247. [CrossRef]
23. Leo, F.D.; Briganti, R.; Besio, G. Trends in ocean waves climate within the Mediterranean Sea: A review. *Clim. Dyn.* **2023**. [CrossRef]
24. Taylor, K.E.; Stouffer, R.J.; Meehl, G.A. An Overview of CMIP5 and the Experiment Design. *Bull. Am. Meteorol. Soc.* **2012**, *93*, 485–498. [CrossRef]
25. Döscher, R.; Acosta, M.; Alessandri, A.; Anthoni, P.; Arsouze, T.; Bergman, T.; Bernardello, R.; Boussetta, S.; Caron, L.P.; Carver, G.; et al. The EC-Earth3 Earth system model for the Coupled Model Intercomparison Project 6. *Geosci. Model Dev.* **2022**, *15*, 2973–3020. [CrossRef]
26. Morim, J.; Hemer, M.; Cartwright, N.; Strauss, D.; Andutta, F. On the concordance of 21st century wind-wave climate projections. *Glob. Planet. Chang.* **2018**, *167*, 160–171. [CrossRef]
27. Oppenheimer, M.; Glavovic, B.; Hinkel, J.; van de Wal, R.; Magnan, A.; Abd-Elgawad, A.; Cai, R.; Jara, M.C. Sea Level Rise and Implications for Low-Lying Islands, Coasts and Communities. In *IPCC Special Report on the Ocean and Cryosphere in a Changing Climate*; Technical Report; IPCC: Cambridge, UK; New York, NY, USA, 2019; pp. 321–445.
28. Ulazia, A.; Saenz-Aguirre, A.; Ibarra-Berastegui, G.; Sáenz, J.; Carreno-Madinabeitia, S.; Esnaola, G. Performance variations of wave energy converters due to global long-term wave period change (1900–2010). *Energy* **2023**, *268*, 126632. [CrossRef]
29. Ulazia, A.; Esnaola, G.; Serras, P.; Penalba, M. On the impact of long-term wave trends on the geometry optimization of oscillating water column wave energy converters. *Energy* **2020**, *206*, 118146. [CrossRef]
30. Simonetti, I.; Cappietti, L. Effects of projected wave climate changes on the sizing and performance of OWCs: A focus on the Mediterranean and Atlantic European coastal waters. In Proceedings of the European Wave and Tidal Energy Conference, Bilbao, Spain, 3–7 September 2023; Volume 15. [CrossRef]
31. Caires, S.; Yan, K. Ocean surface wave time series for the European coast from 1976 to 2100 derived from climate projections. In *Copernicus Climate Change Service (C3S) Climate Data Store (CDS)*; Technical Report; ECMWF: Reading, UK, 2020. [CrossRef]
32. Hersbach, H.; Bell, B.; Berrisford, P.; Hirahara, S.; Horányi, A.; Muñoz-Sabater, J.; Nicolas, J.; Peubey, C.; Radu, R.; Schepers, D.; et al. The ERA5 global reanalysis. *Q. J. R. Meteorol. Soc.* **2020**, *146*, 1999–2049. [CrossRef]
33. ECMWF. *IFS Documentation CY41R2–Part VII: ECMWF Wave Model*; Technical Report; ECMWF: Reading, UK, 2016. [CrossRef]
34. ECMWF. *Product User Guide for Sea Level and Ocean Wave Products—Time Series and Indicators—C3S-422-Lot2-Deltares—European Services, Official Reference*; Technical Report, ECMWC Coperincus Report; ECMWF: Reading, UK 2019.
35. Sheng, W.; Li, H. A Method for Energy and Resource Assessment of Waves in Finite Water Depths. *Energies* **2017**, *10*, 460. [CrossRef]
36. Sen, P.K. Estimates of the Regression Coefficient Based on Kendall's Tau. *J. Am. Stat. Assoc.* **1968**, *63*, 1379–1389. [CrossRef]
37. Kendall, M.G. A New Measure of Rank Correlation. *Biometrika* **1938**, *30*, 81–93. [CrossRef]
38. Lavidas, G.; Venugopal, V.; Friedrich, D. Wave energy extraction in Scotland through an improved nearshore wave atlas. *Int. J. Mar. Energy* **2017**, *17*, 64–83. [CrossRef]
39. Kamranzad, B.; Lavidas, G.; Takara, K. Spatio-Temporal Assessment of Climate Change Impact on Wave Energy Resources Using Various Time Dependent Criteria. *Energies* **2020**, *13*, 768. [CrossRef]
40. Lavidas, G.; Kamranzad, B. Assessment of wave power stability and classification with two global datasets. *Int. J. Sustain. Energy* **2020**, *40*, 514–529. [CrossRef]
41. Kamranzad, B.; Lin, P.; Iglesias, G. Combining methodologies on the impact of inter and intra-annual variation of wave energy on selection of suitable location and technology. *Renew. Energy* **2021**, *172*, 697–713. [CrossRef]
42. Cornett, A.M. A global wave energy resource assessment. In Proceedings of the Proceedings of the Eighteenth (2008) International Offshore and Polar Engineering Conference, Vancouver, BC, Canada, 6–11 July 2008.
43. Vannucchi, V.; Cappietti, L. Wave Energy Assessment and Performance Estimation of State of the Art Wave Energy Converters in Italian Hotspots. *Sustainability* **2016**, *8*, 1300. [CrossRef]
44. Rusu, L.; Onea, F. The performance of some state-of-the-art wave energy converters in locations with the worldwide highest wave power. *Renew. Sustain. Energy Rev.* **2017**, *75*, 1348–1362. [CrossRef]
45. Bozzi, S.; Besio, G.; Passoni, G. Wave power technologies for the Mediterranean offshore: Scaling and performance analysis. *Coast. Eng.* **2018**, *136*, 130–146. [CrossRef]
46. Kamranzad, B.; Hadadpour, S. A multi-criteria approach for selection of wave energy converter/location. *Energy* **2020**, *204*, 117924. [CrossRef]
47. Majidi, A.G.; Bingölbali, B.; Akpınar, A.; Rusu, E. Wave power performance of wave energy converters at high-energy areas of a semi-enclosed sea. *Energy* **2021**, *220*, 119705. [CrossRef]
48. Weinstein, A.; Fredrikson, G.; Parks, M.K.N. AquaBuOY-the offshore wave energy converter numerical modeling and optimization. In Proceedings of the Oceans '04MTS/IEEEtechno-Ocean'04, Kobe, Japan, 22–26 September 2004. [CrossRef]
49. Dunnett, D.; Wallace, J.S. Electricity generation from wave power in Canada. *Renew. Energy* **2009**, *34*, 179–195. [CrossRef]
50. Sinden, G. *Variability of UK Marine Resources, Carbon Trust Report*; Technical Report; Environmental Change Institute: Oxford, UK, 2005.
51. Veigas, M.; López, M.; Romillo, P.; Carballo, R.; Castro, A.; Iglesias, G. A proposed wave farm on the Galician coast. *Energy Convers. Manag.* **2015**, *99*, 102–111. [CrossRef]

52. Pecher, A.; Kofed, G.; Espedal, J.; Hagberg, S. Results of an Experimental Study of the Langlee Wave Energy Converter. In Proceedings of the Twentieth (2010) International Offshore and Polar Engineering Conference, Beijing, China, 20–25 June 2010.
53. Falcão, A.F.; Henriques, J.C. Oscillating-water-column wave energy converters and air turbines: A review. *Renew. Energy* **2016**, *85*, 1391–1424. [CrossRef]
54. Aquafact. *Marine Environmental Appraisal of an Ocean Energy Test Site in Inner Galway Bay*; Technical Report; Hydraulics and Maritime Research Centre, University College Cork: Cork, Ireland, 2010.
55. Simonetti, I.; Cappietti, L.; Elsafti, H.; Oumeraci, H. Optimization of the geometry and the turbine induced damping for fixed detached and asymmetric OWC devices: A numerical study. *Energy* **2017**, *139*, 1197–1209. [CrossRef]
56. Babarit, A.; Hals, J.; Muliawan, M.; Kurniawan, A.; Moan, T.; Krokstad, J. Numerical benchmarking study of a selection of wave energy converters. *Renew. Energy* **2012**, *41*, 44–63. [CrossRef]
57. Johan, A.O.; Magnar, R.; Øyvind, B.; Elzbieta, B.G.; Lars, I.E.; Odin, G.; Karin, M.A.; Bent, N.; Erik, V. Projected changes in significant wave height toward the end of the 21st century: Northeast Atlantic. *J. Geophys. Res. Ocean.* **2017**, *122*, 3394–3403. [CrossRef]
58. Lobeto, H.; Semedo, A.; Menendez, M.; Lemos, G.; Kumar, R.; Akpinar, A.; Dobrynin, M.; Kamranzad, B. On the assessment of the wave modeling uncertainty in wave climate projections. *Environ. Res. Lett.* **2023**, *18*, 124006. [CrossRef]
59. Loarca, A.L.; Berg, P.; Giovanni, A.B.B. On the role of wave climate temporal variability in bias correction of GCM-RCM wave simulations. *Clim. Dyn.* **2023**, *61*, 3541–3568. [CrossRef]
60. Lobeto, H.; Menendez, M.; Losada, I.J. Projections of Directional Spectra Help to Unravel the Future Behavior of Wind Waves. *Front. Mar. Sci.* **2021**, *8*, 655490. [CrossRef]
61. Lavidas, G.; Venugopal, V. A 35 year high-resolution wave atlas for nearshore energy production and economics at the Aegean Sea. *Renew. Energy* **2017**, *103*, 401–417. [CrossRef]
62. Aristodemo, F.; Algieri Ferraro, D. Feasibility of WEC installations for domestic and public electrical supplies: A case study off the Calabrian coast. *Renew. Energy* **2018**, *121*, 261–285. [CrossRef]
63. Bozzi, S.; Archetti, R.; Passoni, G. Wave electricity production in Italian offshore: A preliminary investigation. *Renew. Energy* **2014**, *62*, 407–416. [CrossRef]
64. Mérigaud, A.; Ringwood, J.V. Power production assessment for wave energy converters: Overcoming the perils of the power matrix. *Roceedings Inst. Mech. Eng. Part M J. Eng. Marit. Environ.* **2018**, *232*, 50–70. [CrossRef]
65. Simonetti, I.; Crema, I.; Cappietti, L.; Oumeraci, H. Site-specific optimization of an OWC wave energy converter in a Mediterranean area. In *Progress in Renewable Energies Offshore*; Soares, C.G., Ed.; Taylor & Francis Group: London, UK, 2016. [CrossRef]
66. Kardakaris, K.; Boufidi, I.; Soukissian, T. Offshore Wind and Wave Energy Complementarity in the Greek Seas Based on ERA5 Data. *Atmosphere* **2021**, *12*, 1360. [CrossRef]
67. Abu Zed, A.A.; Kansoh, R.M.; Iskander, M.M.; Elkholy, M. Wind and wave climate southeastern of the Mediterranean Sea based on a high-resolution SWAN model. *Dyn. Atmos. Ocean.* **2022**, *99*, 101311. [CrossRef]